DESIGN AND CONSTRUCTION OF A PORTABLE NEUTRON RADIOGRAPHIC CAMERA

by

Dursun Akbulut

B.S. in Physics, Atatürk University, 1980

Submitted to the Institute for Graduate Studies in Science and Engineering in partial fulfillment of the requirements for the degree of

Master of Science

in

Nuclear Engineering

Boğaziçi University

1984

DESIGN AND CONSTRUCTION OF A PORTABLE NEUTRON RADIOGRAPHIC CAMERA

APPROVED BY

Prof.Dr.T.B.Enginol
(Thesis Supervisor)
Doç.Dr.A.Nezihi Bilge

Doç.Dr.Ergin Kısakürek

Doç.Dr.Vural Altın

DATE OF APPROVAL 1.6.1984

ACKNOWLEDGEMENT

Special thanks to Prof. Dr. T.B.Enginol for his continual help and guidance throughout this work, I would also like to express my gratitude to Doç.Dr.Ali Nezihi Bilge and Doç.Dr.Vural Altın for their helpful discussions.

ABSTRACT

The subject of this thesis is to provide a coherent picture of the components and methods involved in neutron radiography, that is by now a proven technique in non destructive testing.

Having presented a detailed picture of the principles related to neutron radiography, design and construction of a neutron radiographic camera, containing a ^{241}Am - Be neutron source has been developed.

In the first chapter the methods and components of a neutron radiography unit has been described.

In chapters two, three, four and five the components of neutron radiographic facility has been considered in a detailed manner.

In chapter six the design of a neutron radiographic camera has been considered and some theoretical methods have been applied to determine the thermal neutron distribution and the dose rates.

Finally, construction of a neutron radiographic camera and discussion of prospects on this topic and applications have been presented in the last section.

ÖZET

Bu çalışmanın konusu, tahribatsız muayene teknikleri arasında denenmiş bir yöntem olan nötron radyografisi prensipleri ve bileşenlerinin detaylı bir biçimde sunumudur.

Nötron radyografisi tekniğinin ayrıntılı tanıtımından sonra ^{241}Am - Be nötron kaynağı içeren bir nötron radyografi kamerasının tasarım ve yapımı gerçekleştirilmiştir.

Birinci bölümde bir nötron radyografi ünitesinin dayandığı yöntem ve bileşenler tanıtıldıktan sonra 2, 3, 4 ve 5 ci bölümlerde böyle bir ünitenin ayrıntıları incelenmiştir. Altıncı bölümde kamera tasarımı amacıyla termal nötron dağılımı ve doz hesaplamaları için gerekli teorik yöntemler uygulanmıştır. Son bölümde ise, bir nötron radyografi kamerasının yapımı ve muhtemel uygulamalar açısından değerlendirilmesi yapılmıştır.

TABLE OF CONTENTS

LIST OF TABLES

LIST OF FIGURES

LIST OF SYMBOLS

σ	Cross section
Σ_s	Total scattering cross section
Σ_a	Total abroption cross section
M_r	Moderation ratio
$\bar{\xi}$	Average logarithmic energy decrement per collision
ϕ	Neutron flux
J	Neutron current
L	Collimator length,diffusion lengt
D	Collimator inlet diameter,dose rate,film density
L_s	Source to object distance
L_f	Image to object distance
U_g	Geometric unsharpness
U_i	Inherent unsharpness
U_t	Total unsharpness
λ	Decay constant
A	Activity
E	Exposure,energy
G	Contrast
λ_{tr}	Transport mean free path
ϕ_f	Fast flux
ϕ_{th}	Thermal flux
Σ_r	Removal cross section
S	Neutron source strength
τ	Age to thermal range
D	Diffusion constant
g	Slowing down density
θ	Angular divergens of collimated beam
f	Attenuation factor of neutrons
B	Build-up factor
S_a	Surface source strength
S_v	Voulemetric source strength
P_1	$E_1(\Sigma_r + K)R$

CHAPTER 1

INTRODUCTION

1.1. The Discovery of Neutron and Its Properties

Neutron was discovered by Chadwick in 1932 when he was investigating the nature of a highly penetrating radiation which resulted when alpha particalesfrom polonium were allowed to bombard beryllium. At that time Bothe and Becker in Germany and Joliet-Curies in Paris were also searching the nature of this highly penetrating radiation. They assumed the beryllium radiation to consist of highly penetrating gamma rays.

However there was a problem, such that the protons produced by the beryllium radiation allowed to bombard paraffin, possesed an energy of approximately 5-7 Mev and the computed value to produce recoil protons with such energy would require incident gamma rays of approximately 55 Mev. So it could'nt be explained how such a high energy gamma ray could be produced by beryllium, bombarded with polonium alpha particles having energies of approximately five Mev.

Chadwick reasoned that momentum and energy must be conserved. In this reaction, so that, if the unknown radiation consisted of particles having a mass of approximately that of proton, then all of the problems disappeared. Then he explaned the nature of the beryllium radiation as an uncharged particle known as neutron and having a mass slightly higher than proton.

As already indicated, the mass of neutron is slightly higher than that of proton, i.e. 1.00807 atomic mass unit, and it possesses no electrical charge. Neutron is an unstable particle with a half life of 12 minutes when it's free from nucleus, and it decays in to a proton, an electron, and a neutrino.

Since neutron carries no charge, it is unaffected by electrostatic fields. Therefore neutrons can easily penetrate the electronic cloud surrounding the nucleus and interract directly with the atomic nucleus.

The probability that a nuclear reaction will occure between neutron and nucleus is measured by its cross section. The unit of microscobic cross section is barn and measured in areal dimensions, i.e. 1b= $10^{-24}cm^2$. The total cross section is equal to the sum of the absorbtion da and scattering cross section, which are elastic and inelastic, σ_s, and varies with the incident neutron energy, and the nuclear structure of the target nucleus. The reaction types between neutron and nucleus will be explained with more detail in the shielding section.

Neutrons are classified in to a number of groups according to their energies. The energy groups and the properties of neutrons in these groups are presented in Table 1.1.

1.2. Neutron Radiography History

Neutron radiography was began shortly after Chadwick's discovery of neutron. Routine radiography began to take place after the first thermal reactor went critical, in the 1960's and 1970's.

The first investigation about neutron radiography was performed in Germany by Kallman, and Khun using small accelerator-type neutron generator. They and other workers, such as Peter in Germany, Thewlis and Derbyshire at Harwell showed that neutron radiography has some advantages over x-radiography for sepacial and difficult inspection problems.

After the development of available neutron sources, neutron radiography was mostly done in research centers, and came in to real use in the inspection of nuclear fuel.

Around 1970's some of neutron radiography centers were opened in U.S.A. and European countries, so that outside industries could send them any item they wished to have neutron radiographed.

Then some standards were established, as neutron radiography took its place along side other non destructive testing techniques.

Now, centers with considerable needs for neutron radiography are beginning to purchase and optimize their own radiography facilities for their own work scattered around in the world. In addition some trends are

TABLE 1.1. Neutrons Classified According to Energy (2).

Term	Comments	Energy range
Slow		0.00eV to 10^3eV
Cold	Materials possess high cross-sections at these energies, which decrease the transparency of most materials but also increase the efficiency of detection. A particular advantage is the reduced scatter in materials at energies below the Bragg cutoff.	Less than 0.01 eV
Thermal	Produced by slowing down of fast neutrons until the average energy of the neutron is equal to that of the medium. Thermal neutrons provide good discriminatory capability between different materials; sources are readily available.	0.01 eV to 0.3eV
Epithermal	Produced at energies greater than thermal, e.g. fission energies and surrounded by a moderator. Neutrons are slowed down until they have energies in thermal equilibrium with the moderator molecules. At any location where thermal equilibrium has not been achieved the distribution of neutron velocities will contain velocities that exceed that permitted by a Maxwellian distribution of the moderator temperature. Such neutrons are referred to as epithermal neutrons.	0.3 eV to 10^4eV
Resonance	Certain nuclei exhibit strong absorbtion characteristics at well-defined energies called resonance absorptions. Neutrons in these specific energy ranges are referred to as resonance neutrons and provide excellent discrimination for particular materials by working at energies of resonance. Greater transmission and less scatter occur in samples containing materials such as hydrogen and enriched reactor fuel materials.	1 eV to 10^2eV
Fast	Fast neutrons provide good penetration. Good point sources of fast neutrons are available. At the lower energy end of the spectrum fast neutron radiography may be able to perform many inspections performed with thermal neutrons, but with a panoramic technique. Poor material discrimination occurs, however, because the cross-sections tend to be small and similar.	10^3eV to 20MeV
Relativistic		>20 MeV

developing to look beyond the capabilities of a straight forward thermal neutron radiography (2).

1.3. Basic Types of Applications of Neutron Radiography

To understand the capabilities of neutron radiography applications it will be useful to view the capabilities of neutron radiography in comparison with that of x-radiography, this is because, neutron radiograp and x- radiography are similar in the principle of their techniques. From Figure 1.1 one see that thermal neutrons show a random attenuation pictur with regularly increasing atomic number of absorber. The x-ray attenuatio coefficient, on the other hand, increases in regular manner when similarl

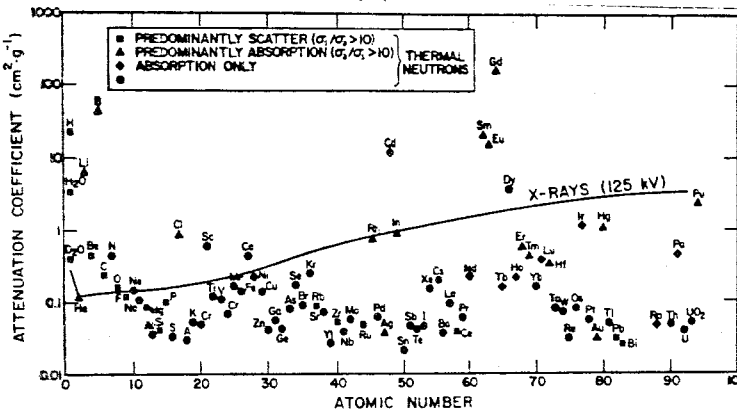

Fig. 1.1. A Comparison of mass-attenuation coefficients of the elements for X-rays (solid line) and for thermal neutrons plotted as a function of atomic number of absorber (1).

examined. At low energies neutrons show relatively more attenuation than x-rays for low atomic number materials. Conversely thermal neutrons are transmitted easily by most heavy materials. But x-rays are absorbed strongly. This major difference in attenuation characteristics pre sents a major attraction for successfull examination of plastic, rubber, paper, adhesive, explosive, i.e. high hydrogen content materials, in metal containment assemblies. Also the use of radiography to discriminate betwe many neighboring elements is easier with thermal neutrons than it is with x-rays. For example, in discriminating between carbon and boron, cadmium and barium with thermal neutron radiography, presents less difficulty than x-ray radiography does.

On the other hand, it is possible to differentiate the isotopes the same element with neutron radiography, be cause the attenuation of neutrons by different isotopes can be quite different.

In general neutron radiography has following potential applicatio a) Radiography of dense materials b) Contrast of light materials envelop in denser materials c) Contrast between isotopes of the same element d) Radiography of radioactive materials f) Biomedical applications.

1.4. Neutron Radiography and Its Components

As in all forms of radiography neutron radiography consists of placing an object in a neutron beam and recording the emerging neutron beam, which can become spatially hetro geneous according to the isotopi composition of the object, by means of suitable detectors. The differenc from other forms is such that the emerged neutrons are first absorbe by converter material which then emits secondary radiation that in turn contributes to the formation of a direct or indirect latent image in a suitable recorder. The latent image eventually made visible to the naked eye in the form of spatially varying darkness or tracs, and can be relate to the material composition of the object to yield desired material infor tion.

Most of neutron radiography is made with thermal neutron because, as already indicated before, this is the energy region that exhibits the most interesting, and useful attenuation characteristics. Also thermal neutron images easiest to detect and record. There are some applications in which resonance, fast and cold neutrons are necessary. But we will mostly be concerned with thermal neutron radiography.

Since most of neutrons are born in a suitable source with energie considerably above thermal, moderation of neutrons is necessary for therm neutron radiography. After moderation, the moderated neutrons diffuse in all directions, hence some selection of neutrons is necessary in order to obtain a sharp radiography of the object. It is the function of collimato that performs this selection. Then to record the attenuated beam a detec- tion system is necessary, and finally a biological shield must employed for reasons of safety.

The main components of neutron radiographic imaging system is shown schematically in Figure 1.2.

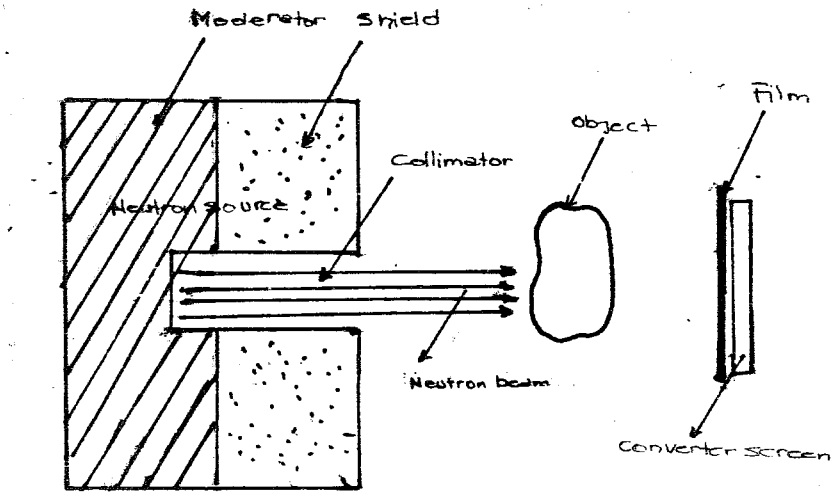

Fig. 1.2. Graphical representation of neutron radiographic syst

1.5. Scope

In the first part of this thesis neutron radiography is described as a Non Destructive Testing tool. Attention has been concentrated on thermal neutron radiography and the components of neutron radiography systems are given in a detailed manner, in Chapters 2, 3, 4, 5. In Chapter 6 the design of a neutron radiography camera is presented. In Chapter 7 the construction of a practical camera containing ^{241}Am-Be neutron source, for use in laboratory, is presented.

CHAPTER II

NEUTRON SOURCES

Neutron sources are classified in to three general types a) nuclear reactors b) accelerators c) radioactive isotopes.

The possible use of these neutron sources for neutron radiography must be considered from several point of view. One must consider the neutron energy and intensity, gamma intensity, cost, size, portability, shielding problemsand general utility. Each of these characteristics for each of neutron sources will be considered and finally be compared.

2.1. Reactor Neutron Sources

Although most reactor based neutron radiography facilities use research reactors which have been installed for a variety purposes, there are many reactors that are installed specifically for neutron radiography.

Any nuclear reactor equipped with probe tubes and capable of operat at a power greater than one Kw can be useful for neutron radiography. However higher power leads to greater source flux, hence the more convenie the methods, and the better the radiagraphs become. Generally research reactors have the thermal flux intensity range of 10^{12} to $5x10^{14}$ n/cm^2-sec^{-1} with their thermal output of 250 Kw to 50 mw and have 10 to 20 beam facilities. Any of these beam facilities can be employed for neutron radiography with minor modifications.

In recent years the steadly increasing demand for neutron radiograp especially for special problems such as those involved in the shipment of explosives or reactor fuel, has led to the development or a series of small simple, and relatively inexpensive reactors designed primarily for neutron radiography. Such reactors operate at a power range of 5 to 250 Kw, and in thermal flux range of $2.5x10^{11}$ to 10^{13} n/cm^2-sec with relatively low costs(Some of these type reactors are TRIGA, CANADA SLOW POKE-2, COMMISSARIATE Al ENERGIE ATOMIQUE reactors (4).

2.2. Accelerator Neutron Sources

A large number of neutrons are produced by bombarding suitable target materials with accelerated positive ions. Typical reactions are

$$^{9}_{4}Be + ^{2}_{1}D \rightarrow ^{10}_{5}B + n + 4.35 \text{ MeV}$$
$$^{2}_{1}D + ^{2}_{1}D \rightarrow ^{4}_{2}He + n + 3.28 \text{ MeV}$$
$$^{3}_{1}T + ^{2}_{1}D \rightarrow ^{4}_{2}He + n + 17.6 \text{ MeV}$$
$$^{9}_{4}Be + ^{2}_{1}H \rightarrow ^{9}_{5}B + n + 1.85 \text{ MeV}$$
$$^{9}_{4}Be + \gamma \rightarrow 2^{4}_{2}He + n - 1.67 \text{ MeV}$$

Fig. 2.1 shows the neutron yield as a function of positive ion energy from several of these reactions.

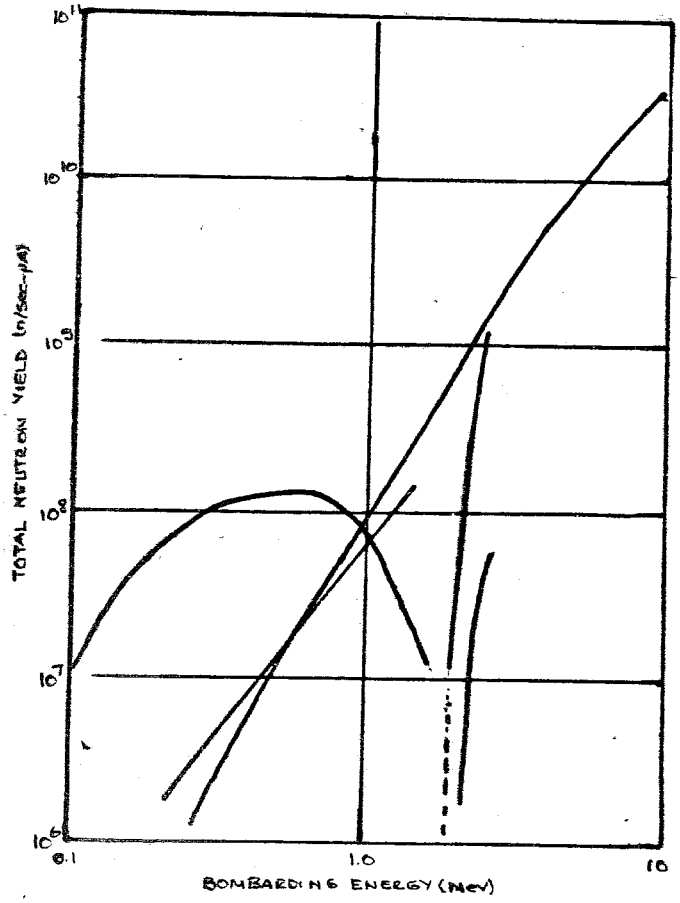

Fig. 2.1. Total neutron yield versus bombarding energy for several accelerator produced neutron reactions (5).

In addition to the neutron yield, the energy spectrum of the sourc neutrons is also important, since the higher the neutron energy the great the average distance it may travel in a moderator before becoming thermalized. Hence the thermal flux distribution produced by higher energ neutron sources will be necessarily more dispersed than that of a low energy source, and the maximum peak flux will be lower. To compare differ sources with this respect, the thermalization factor of some sources in water are given in Table 2.1.

TABLE 2.1. Some Thermalization Factors Measured in Water Moderator (3).

Source	Thermalization Measured	Factor Rounded
D(d,n) at 150 kev	196	200
T(d,n) at 150 kev	645	650
Be(p,n) at 2.8 Mev	38	40
Be(d,n) at 2.8 Mev	298	300

Among these reactions $^{3}H(d,n)^{4}He$,D-T reaction has received the mos attention, because it has relatively high yield at low bombarding energie In this type reaction accelerating voltates are in the order of 150 to 40 kilovolts whereas the other reactions require accelerating voltages in th order of Mev range. Lower bombarding energies for D-T reaction have made it economically useful. A fast neutron output of order off 10^{11}-10^{12}n/s can be obtained from this reaction. Sealed tube neutron generators employ this type reaction. From radiographic point of view, the disadvantage of the D-T reaction neutron source are such that, it produces neutrons of relatively high energy, and tritium targets have short life time. The target has an endurance of hundred hours before the titanium target surfa becomes too demaged to hold tritium. However the high energy, 14 mev, of neutrons can be used to induce fast fission in uranium, An improvement in the peak thermal flux by a factor of around 2.5 was obtained when 2.5 cm thick natural uranium is placed in front of the target (3), (6).

The $Be(d,n)^{10}B$ reaction has the highest neutron yield for positive ion bombardment. However energies in excess of 1 Mev are necessary to obtain such high yield. Expensive and bulky equipment, such as Van de Graff accelerators are needed to supply accelerating potential of this magnitud But this and other positive ion neutron yielding reactions which require

acceleration voltages in the Mev region have some advantages in that such generators are more versatile. For example these machines are often capable of accelerating different projectiles employing different targets, such as Be(d,n) and Be(p,n) (5).

One other type of reaction is the photo neutron (x,n) reaction caused by use of irradiating a suitable neutron yielding material with the bremstrahlung produced when energetic electrons strike a target of high atomic number. Therefore an electron accelerator equipment (electron linear accelerator) can be used as a neutron source. As a target element for such equipment, any nuclide can be made to undergo photo desintegration with photons of adequate energy. Most of the target materials require photons of greater than eight Mev energy except beryllium, 1.66 Mev, and deuterium 2.2 Mev. Uranium and beryllium are most widely used target materials. The threshold of uranium is ∿9 Mev and yield reises quite rapidly as photon energy increases. Accelerators that produce such high energy x-rays for photo neutron production serves dual role, since it could be used for neutron radiography for high energy x-radiography (5).

2.3. Radioisotope Neutron Sources

Radioisotope neutron sources are based on the (α,n) reaction with beryllium and boron as the standart target, on photo neutron or (γ,n) reaction with beryllium and deuterium (D_2O) as the target, or on spontaneous fission with heavy nuclei, such as ^{252}Cf being widely used. The characteristics of some of radioisotope neutron sources are given in Table 2.2 and some of reactions are

$$Be + \alpha \rightarrow C + n + 5.71 \text{ Mev}$$
$$Be + \gamma \rightarrow 2\ \alpha + n - 1.67 \text{ Mev}$$
$$H + \gamma \rightarrow H + n - 2.33 \text{ Mev}$$
$$^{252}Cf \rightarrow 2 \text{ fiss} + 3.8\ n + 200 \text{ Mev}$$

(α,n) sources: The most commonly employed alpha emitters are ^{241}Am, ^{239}Pu, ^{210}Po and ^{226}Ra having alpha energies of 5.477, 5.114, 5.305, 4.777 Mev. A common neutron source is prepared by a mixture of an alpha emitter and a light element, such as Be. Among these sources Pu forms intermetallic compounds with Be wheras in the case of radium and polonium it is necessary

to prepare pressed mechanical mixtures.

The mixture or compound is doubly encapsulated, first in a welded inner capsule of Ta, then in stainless stell (see Fig. 2.2)

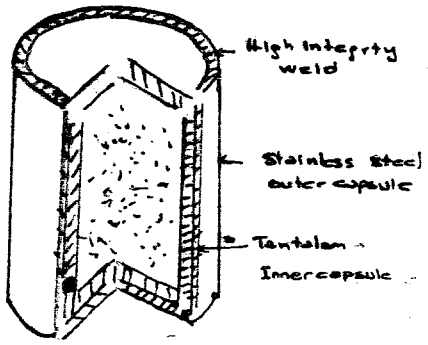

Fig. 2.2. Standart Numec Plutonium-Beryllium neutron source (7).

The practical neutron yield depends on the physical and chemical properties of the mixture. Energy spectrum of the neutrons can be calculat on the basis of Q, energy change due to the differency in total rest masse of all constituents of the reaction, kinematics of (α,n) reaction and the nuclear properties of ^{9}Be. However, the neutrons are not mono energetic because alpha particles lose energy in the material and all angles of incidence are experinced. (7), (9).

(γ,n) Sources : Since the γ energy of radioactive substances rarely exceed 3 Mev only beryllium and deuterium are used as target elements. The Q valu of $^{9}Be(\gamma,n)$ and $^{2}D(\gamma,n)$ reactions are 1.67 MeV and 2.23 MeV respectively.

The most commonly used photo neutron source is ^{124}Sb-Be which producesneutron of 26 kev energy. Antimony-124 is produced by irradiation of normal antimony.

Spantaneous Fission Sources : The even mass isotopes with the heavist even-Z elements are spontaneously fissioning elements. Among these Californium-252 is the most commonly used isotope because of its high neutron output, and it is produced in milligram to gram quantities by irradiation of plutonium, or transplutonic nucleidesin high thermal neutron fluxes. This source is being increasingly used as radioactive neutron source for radio-

TABLE 2.2. Characteristics of Some Radioactive Neutron Sources (3).

ISOTOPE	HALF-LIFE	NEUTRON PRODUCING REACTION	NEUTRON YIELD($n \cdot s^{-1}$) Per ci	Per g	APPROXIMATE MEAN ENERGY (MEV)	γ-RADIATION FROM EN CAPSULATED SOURCE ENERGY	EXPOSURE LATE Per 10^8 n SEc^{-1}	HEAT OUTPUT ($W/10^8 ns^{-1}$)
^{242}Cm	163 d	$^{9}_{4}Be(\gamma,n)^{12}_{4}C$	25×10^6	8.5×10^9	4-6	< 0.04 most abundant	0.04	1.5
^{228}Th	1.91 a	$^{9}_{4}Be(\gamma,n)^{12}_{6}C$	2×10^7	1.7×10^{10}	4-6	Various up to 2.6(max)	3	1.0
^{252}Cf	2.65 a	Spontaneous fission	4.3×10^9	2.3×10^{12}	2	0.5 to 1 most abundant	0.007	0.001
^{244}Cm	18.1 a	$^{9}_{4}Be(\gamma,n)^{12}_{6}C$	2.5×10^6	2.1×10^8	4-6	0.043 most abundant	negligible	1.4
^{227}Ac	21.8 a	$^{9}_{4}Be(\gamma,n)^{12}_{6}C$	1.5×10^7	1.1×10^9	4-6	Various up to 0.83(max)	0.8	1.2
^{238}Pu	86.4 a	$^{9}_{4}Be(\gamma,n)^{12}_{6}C$	2.3×10^6	4.1×10^7	4-6	0.099 most abundant	negligible	1.4
^{241}Am	458 a	$Be(\gamma,n)^{12}_{6}C$	2.2×10^6	7×10^6	4-6	0.06	0.1	1.4
^{226}Ra	162 a	$Be(\gamma,n)^{12}_{6}C$	1.3×10^7	1.3×10^7	4-6	Various up to 2.4-0.61 most abundant	6	1.2
$^{124}Sb^{d}$	60 d	$Be(\gamma,n)^{12}_{6}C$	$13.\times10^6$	-	0.024	1.69 most abundant	80	0.04

graphy because its low γ output, yield per unit cost and thermalization factor.

It is worth to mention ^{242}Cm-Be source such that it can be made simply by irradiading an ^{241}Am-Be source in a suitably high flux to produce the Americium-Berillium-Curium source if only 10% of the ^{241}Am in converted to ^{242}Cm the source output is measured by a factor greater than 100 due to the higher α-activity of curium. But the disadvantage is the short half-life of 163 d of Curium. (3).

From the point of view of radiography (γ,n) reaction neutron sources are not useful for neutron radiography because of short half life, small yield of neutrons and high gamma intensity. But (γ,n) sources, especially Sb-Be, yield very low energy neutrons which has an advantage of easy thermalization. The (γ,n) and spontaneous fissioning neutron sources are very useful because of their long-half life and low gamma intensity. Some characteristic comparisons of some radioactive neutron sources for radiograhpy are given in the Table 2.3.

TEBLE 2.3. Characteristics of Some Isotopic Sources for Neutron Radiography(1).

ISOTOPE	REACTION	HALF -LIFE	COMMENTS
^{124}Sb-Be	γ-N	60 days	Short half-life and high γ-background low neutron energy is advantage for thermalization, a low cost, high yield source
^{210}Po-Be	(γ,n)	138 days	Short half life, low γ-background low cost
^{241}Am-Be	(γ,n)	458 a	Long half-life, high cost, easily shielded γ-background
^{241}Am-^{242}Cm-Be	(γ,n)	163 days	Short half-life, medium cost, high neutron yield
^{252}Cf	Spontaneous fission	865 a	Long half-life, high neutron yield, small size and low energy offer advantages in thermalization

The output of a radioactive neutron source can be increased by placing it in a subcritical assembly. This assembly consists of a mixture of moderator and fuel material enriched in ^{235}U. This assembly increases neutron population through fission reaction between thermalized neutrons and ^{235}U nuclei. However, the considerable increase in neutron output depends on critically factor, k_{eff} of the assembly. From Figure 2.3 one can see that k_{eff} must be greater than about 0.9 before a useful increase in neutron output is attained. The studies has been performed on subcritical boosters for neutron radiography at several different laboratories and a thermal flux increase by a factor of 30 over the best pure moderator system was obtained (4). Very recently, Idaho Nuclear have designed a facility of k_{eff} 0.999 which is calculated to give a flux boost of 400.

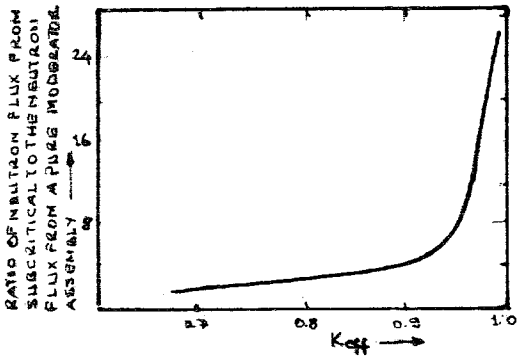

Fig. 2.3. Increase in neutron flux as subcritical size is increased(10).

2.4. Comparison of Neutron Sources

The comparison will be made under the criteria of time required to produce a radiograph, cost and mobility.

The most greatest neutron fluxes are obtained from reactors and most reactor beams are rich in thermal neutrons as compared to the other radiations. This fact is very desirable because neutron radiograhy is mostly done by thermal neutrons. The applications that allow the object to he moved easily generally require either good resolution with low to moderate through put or high production rates, low to moderate resolution and an intense neutron source is highly desirable for either of these conditions. From Table 2.4 cone can see the advantage of reactor neutron sources over all the other sources. On the other hand most of the easly research in neutron radiography has been done in the reactor industry therefore more techniquel back ground is available in this area than radioactive and accelerator sources.

TABLE 2.4. Summary of the Properties of Some Typical Facilities for Neutron Radiography (3).

SOURCE	Collimator Position	Collimator Basic Flux (cm^{-2}-s^{-1})	Typical Beam Characteristics Intensity	L/D	Cd ratio	Imaging Technique[a] Screen	Film[b]	Neutron Exposure Time (S)
Multi-purpose research	Radial	10^{14}	10^{8}	250	2-5	In	D2	10^{2}
reactor	Tangential	10^{13}	10^{7}	250	10-50	Dy	D2	10^{3}
	Cold source	$2x10^{11}$	10^{6}	100	∞	Gd	D2	$2x10^{3}$
Radiography reactor[c]	Radial	10^{12}	10^{6}	250	2-5	In	D2	10^{4}
	Tangential	$4x10^{11}$	$2x10^{6}$	100	10-50	Dy	D4	10^{2}
Be(ϕ,n);3MeV,400μA	Radial	$3x10^{9}$	$2x10^{5}$	33	5-20	Dy	D7	$5x10^{3}$
Be(γ,n);5.5MeV,100μA	Radial	$4x10^{8}$	$8x10^{4}$	18	5-20	Dy	D7	$5x10^{2}$
T(γ,n) U;120keV,7MA	Radial	10^{8}	$2x10^{4}$	18	5-20	Dy	D10	$8x10^{3}$
^{252}Cf;5mg Sub-crit	Radial	$3x10^{9}$	$2x10^{5}$	18	2-10	Dy	D7	$5x10^{3}$
^{252}Cf, 1 mg	Radial	$2x10^{7}$	10^{4}	12	5-20	Gd	D10	$4x10^{3}$

a The transfer technique has been used as the main example here because its value to the nuclear industry. The neutron exposure times assume a film exposure time >5x T 1/2

b Films from the Agfa-Gavent range, other manufacturers offer a closely parallel series of film

c A small reactor designed to make neutron radiography as convenient and economic as possible

The precurement of nuclear reactor requires a big investment because of its expensive licensing and control features. However, on the basis of per neutron output cost, a nuclear reactor will be cheaper than the other two. On the other hand, neutron radiography can be essentially a by-product of many reactors, therefore operating costs can often be shared with other programs. Hence, there are very strong economic incentives to utilize existing facilities whenever possible. One economic way to obtain high intensity thermal flux for neutron radiography is to use a subcritical booster as neutron source. However, the flux advantage is only possible with k_{eff} of 0.9 or greater. Therefore, such an assembly have to have evaluations and approvals for safe guards, operation, and shipping.

In some neutron radiography applications, it is desirable to take the neutron source to the inspection site rather than taking the object to the neutron source, i.e. on-site application is necessary, and modest collimation and lengthy exposure times are acceptable. For such applications, a portable neutron radiography facility, using radioactive neutron source or a small neutron generator is required. Table 2.5 shows the characteristics of neutron sources on the basis of radiographic resolution, exposure speed, ease of operation and economic aspects.

TABLE 2.5. Characteristics of Thermal-Neutron Sources (1).

Type of Source	Typical Radiographic Intensity ($cm^{-2}s^{-1}$)	Radiographic Resolution	Average Exposure Time	Characteristics
Radioisotope	10^1 to 10^4	Poor to medium	Long	Stable operation, medium investment cost, possibly portable
Accelerator	10^3 to 10^6	Medium	Average	On-off operation, medium cost, possibly portable
Subcritical assembly	10^4 to 10^6	Good	Average	Stable, operation, medium to high investment cost Portability difficult
Nuclear reactor	10^5 to 10^8	Excellent	Short	Stable operation, medium to high investment cost Portability, difficult

CHAPTER III

MODERATOR SHILED AND COLLIMATOR

3.1. Moderator

Since all of neutron sources produce fast neutrons, it is necessary to slow down these neutrons to thermal range for thermal neutron radiography. This task is done by the moderator. Moderators must consist of a material that will slow down but not capture neutrons. Materials having high moderation ratio are preffered for this purpose. The moderation ratio is given by

$$M_r = \bar{\xi}\Sigma s/\Sigma a$$

where $\bar{\xi}$ is the average logarithmic energy decrement percollision
Σs is the macroscopic scattering cross section of the medium
Σa is the macroscopic absorbtion cross section of the medium

As will be seen from the formula the moderation ratio is proportional to $\bar{\xi}$ and Σs. However Σ is given by

$$\bar{\xi} = 1 + \frac{(A-1)^2}{2A} \ln \frac{A-1}{A-1}$$

where

A is the atomic weight of the nucleus.

From the formula given above the lower the atomic weight, the greater the $\bar{\xi}$. Therefore as a moderator material, low atomic weight materials or materials containing low atomic weight elements are usually preffered. Such materials are water, heavy water, berylllium, graphite and metalhydrides. From these elements, graphite and other materials with relatively long slowing down lenghts are only appropriate for reactors where primary source is relatively large, and materials with high hydrogen density such as parrafin, water, and metal hydrides should be chosen for radioisotopes and accelerator sources.

3.2. Shield

People working in radiation areas must be protected by shielding against potential hazards arising out of radioactive materials. In nuclear reactors, shields are usually made of a mixture of conerate and heavy materials However for radio isotope and acceleration sources shields are usually made of mixtures of hydrogeneous materials and strong neutron absorbers, such as, boron, lithium.

3.3. Collimator

In neutron radiography, the design of the neutron collimator is an important factor for obtaining good quality radiographs. This importance can be illustrated as in Figure 3.1.

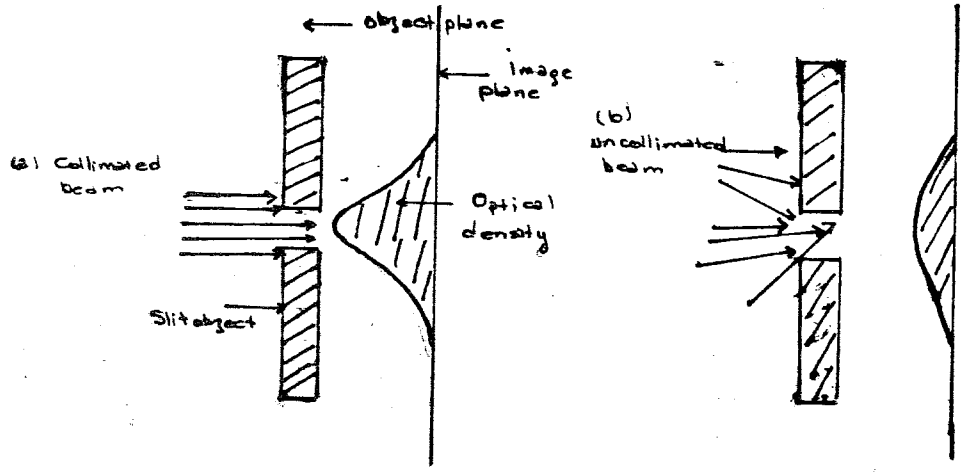

Fig. 3.1. Effect of neutron collimation on image from a slit in neutron absorbing plane.

A well collimated nutron beam, will produce a sharp image while a non collimated neutron beam will not produce such a sharp image.

The collimation of neutrons is made by means of a collimator which is a way of permitting only those neutrons close to the tube to pass to the radiographic position. The walls of the collimator are lined with a neutron opeque materials which prevent stray neutrons entering the system via the collimator wall.

Collimators are classified according to their shape as soller slit (multichannel) paralel sided and divergent collimators as shown in Figure 3.2. (11).

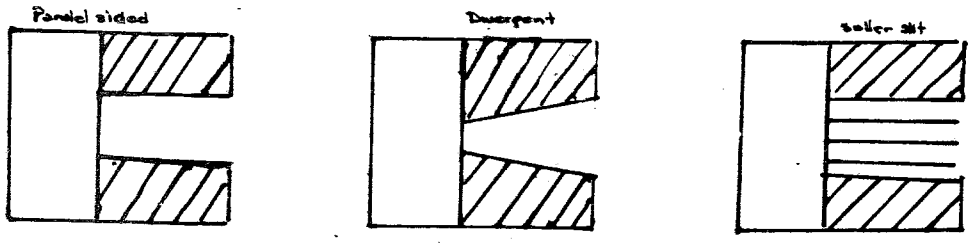

Fig. 3.2. Three types of neutron beam collimators investigated in neutron radiography.

The important factors for each type of collimator are the total length and the size of entrance opening or aperture. These parameters define the angular divergence of the beam and the neutron intensity at the inspected object, as will be seen later.

Each of the collimator systems cited above, has its desirable and undesirable characteristics. The paralel sided collimators produce a beam of parallel path neutrons, but the beam coverage is very limited in size and displaces more moderator material hence reduces the thermal flux. The soller slit collimator provides a larger useful beam area as well as a beam of parallel path neutrons, but the inlet requires a uniform neutron flux over large volume to prevent non uniformity problems at the plane of the inspection object and also producer a pattern of circles or lines on the radiographic image due to a bundle of small tubes or dividing slits

However the divergent collimator can provide a large uniform area on the inspected object but some image distortion occurs at the edge of the inspected object because neutron paths are radial rather than paralel. The beam distortion can be decreased by adjusting collimator dimensions, and the distortion however, is of small interest except in case of a few special inspections. On the other hand the small size of the aperture of the divergent collimator near effective thermal neutron source makes it excellent for small neutron generators and radioactive sources (11).

3.3.1 Assesment of Neutron Beam Intensity

Since we have an isotropic neutron source, the discussion will be concentrated on isotropic neutron sources.

As indicated before, a thermal neutron beam for neutron radiography is obtained from valume distributed sources as show in the Figure 3.3.

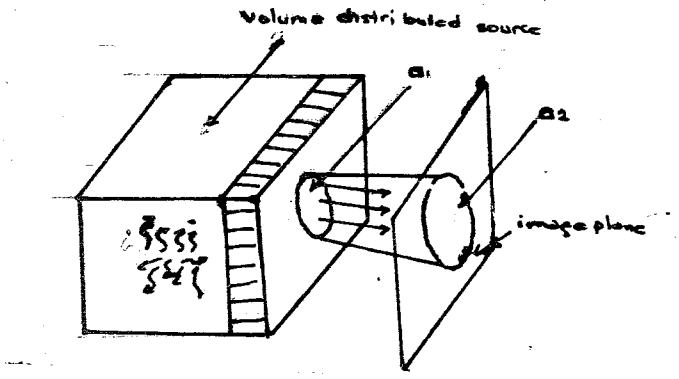

Fig. 3.3. Neutron source, collimator and image plane.

It will be assumed that those neutrons that exit from the volume source and enter the beam tube through the aperture are directionally isotropic. Figure 3.3. describes the system that illustrates the calculation of the neutron intensity at the image plane by the following consturction.

Let ϕ, represent the isotropic neutron flux a the inlet of the collimator, and a, is the inlet aperature area, a_2 is the image plane area, and L is the distance from inlet to collimator to the image plane.

Then the number of neutrons that pass through image area a_2 per second, represented by n is given by

$$n = \phi_1 a_1 \frac{a_2}{4\ \pi L_2} \qquad (3.1.)$$

where $\frac{a_2}{4\ \pi L_2}$ is the fraction of the solid angle subtendet by a_2 at collimator inlet. The neutron flux at the image plane $(cm^{-2} sec^{-1})$ is given by

$$\phi_2 = \frac{n}{a_2} \qquad (3.2)$$

For a circular aperture, $a_1 = \pi(D/2)^2$ yields

$$\phi_2 = \frac{\phi_1}{16} \left(\frac{D}{L}\right)^2$$

where d is the aperture diameter

The fraction of neutrons lost due to collimation will be the ratio

$$\frac{\text{Flux at the entrance}}{\text{Flux at the exit}} = \frac{\phi_1}{\phi_2} = 16 \left(\frac{L}{D}\right)^2 \qquad (3.5.)$$

The ratio of the collimator length to inlet diameter (L/D) is called the collimator ratio which represetens an angular beam divergence θ

$$\theta = \frac{L}{D}$$

This angle is used as a parameter describing the extent of collimation One can see that from equation (3.5.) the larger L/d (smaller θ implies a more collimated beam and the greater loss of intensity at the image surface.

The expression (3.4) was obtained by assuming that all of the neutrons in the collimator orginate at the entrance aperture, but in practice some of them will come from the collimator walls adjacent to the aperture. Howkesworth has shown that the total flux is given by

$$\phi_2 = \frac{\phi_1}{16} \left(\frac{D}{2}\right)^2 \left(1+ \frac{2h}{L}\right) \qquad (3.7.)$$

where h is length of collimator wall which emits neutrons. The length h varies with different types of neutron radiography unit in that it is usually a section of the collimator that is not lined. For sources of low intensity the unlined length is usually about two diameters long. (10)

3.2.2 Control of Important Variables

The location, dimensions and an airgap between collimator and source effects the resolution. the exposure time and the image contrast.

The location of the collimator entrance must be such that it is sufficiently close the source and consistent with the need for enough material for thermalization and attenuation of contaminating radiation. For a radioactive neutron source the location of a collimator entrance in

tangential position will increase the thermal beam intensity and decrease the beam contamination (gamma) and fast neutron flux (because fast and gamma rays, from source itself have a preferential radial direction from the source (see figure 3.4.) This fact improves the resolution and image contrast

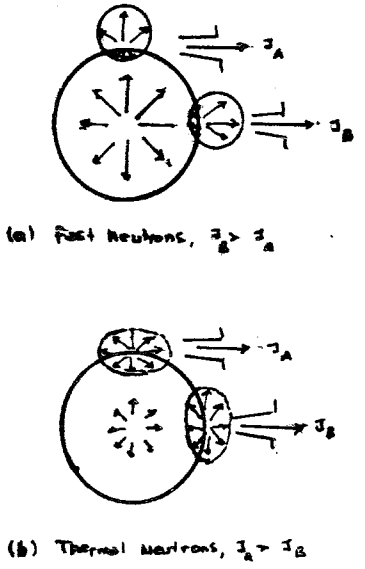

Fig. 3.4. Polar plot representation of fast and thermal neutrons associated with a point source embedded in a moderating medium.

The effect of the collimator dimensions on resolution can be seen from Figure (3.5.) considering the image unsharpness

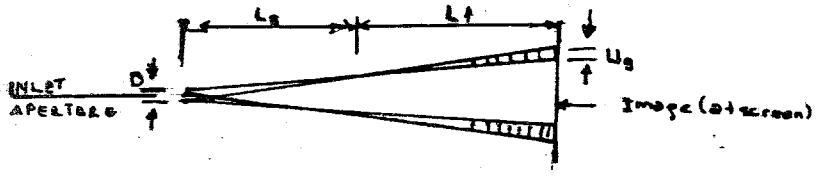

Fig. 3.5. Neutron collimator geometry.

Unsahrpness is expressed by $Ug = \frac{D}{Ls} L_f$

where Ug is the geometric image unsharpness, cm

D is the source-aperture size, cm

L_f is the image to object distance

L_s is the source to object distance

Since $L_f << L_s$ and is usually equal to the object thinkness the geometric unsharpness is linearly dependent the inverse of collimator ratio. So the image unsharpness decreases with ineresing collimator length.

J. Barton have studied the effect of collimator ratio, using radioactive netron source on exposure speed, overall detail visibility and contrast. The effects can be seen from the Figure (3.6.)

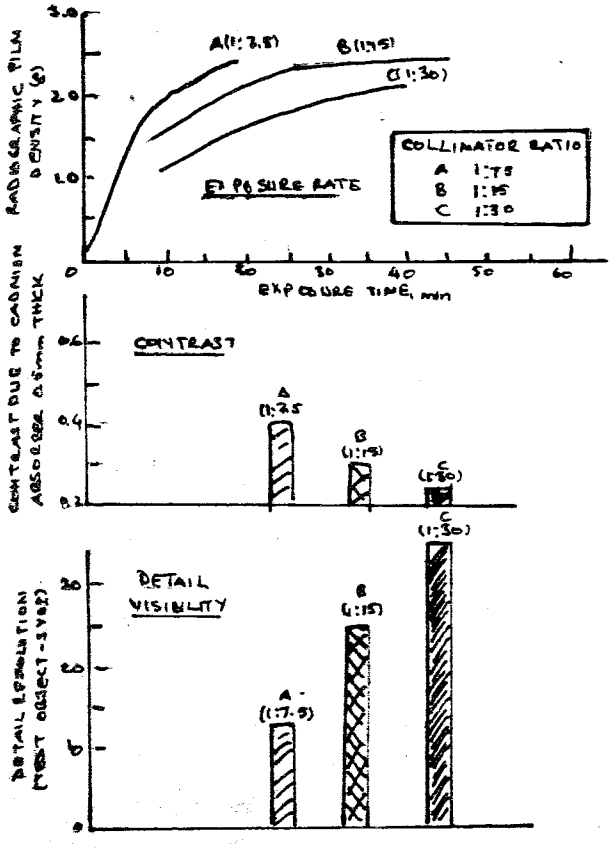

Fig. 3.6. Effects that can be obtained by changing collimator ratio using ^{252}Cf facility (12).

Note that the greater the L/D ratio, the lower the exposure speed, the higher the detail visibility and the lower the contrast.

For a given collimator ratio, the effect of collimator dimensions on exposure time contrast and detail visibility can be seen from Figure (3.7).

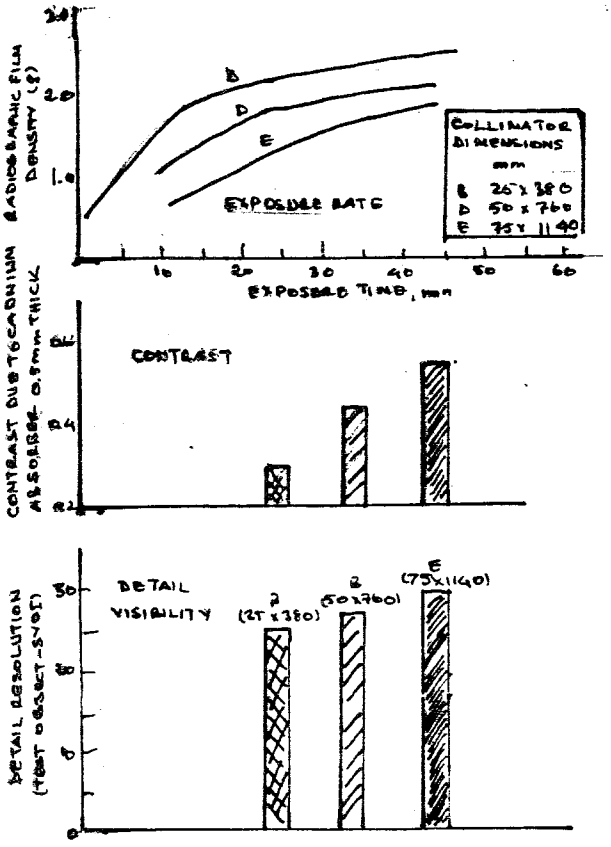

Figure 3.7. Effects that can be obtained by changing collimator dimensions Using ^{252}Cf facility dimensions (collimator ratio held constant), (12).

From Figure 3.7. one can see that a small collimator length with a small aperture D leads to high exposure speed but low contrast. The reasons can be explained by (a) size of input aperture relative to the thermal flux peak in moderator (b) source flux depression caused by large aperture collimators, and (c) interference radiation that reaches the imaging plane (12).

On the other hand, J.P. Barton has shown that an air gap between neutron source and collimator (Figure 3.8.) improves overall detail visibility and increases the exposure speed. This advantage is due to the separation of the highly absorbing collimator material from the peak thermal flux position which leads to reduced thermal flux.

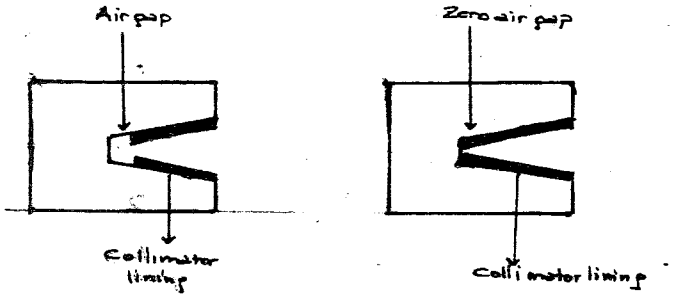

Fig. 3.8. Illustration of air-gap and zero air-gap.

Figure 3.9. shows the effect of changes in the dimension of this air-gap on over all detail visibility, thin object resolution, contrast and exposure speed

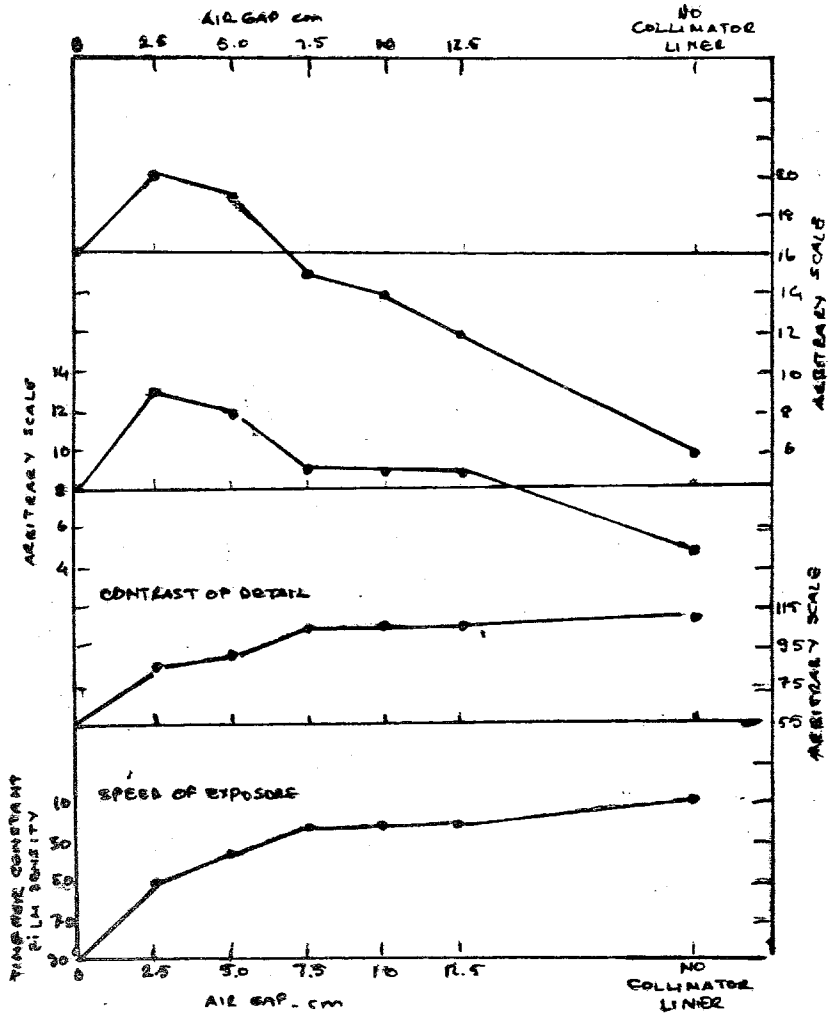

Fig. 3.9. Effects that can be obtained by fine tuning of air-gap.

Note that introducing an air gap leads to approximately 90 percent increase in exposure speed for the first 2.5 cm gap. There after a leveling off trends to occure. Likewise the same effect can be seen on the contrast. However, after 2.5 cm air-gap the resolution sharply increases.

An optimum air-gap is chosen according to the requirentments of each specific application. For over all detail visibility an air gap of 2.5 cm, for the best contrast and exposive speed, 10 cm is recomended and for a good compromise, 5 cm should be used (13)

In generaly, the shape and dimension of a collimator depends on the information of the source and the sample to be radiographed. For reactor sources the dimensions of collimator are usually large and the collimator is lined along its full length (10).

Since the spatial neutron flux in a small source moderator, radioactive and accelator sources, varies across the collimator aperture, and the longer the collimator the greater is the attenuation loss due to collimator atmosfer, for this type of source the collimator is usually made short and narrow. The measure of collimator dimensions is usually a compromise between exposure speed and resolution. But the construction of the neutron source usually sets the limits on the width and the length of a collimator. Generally, it is usual to design collimators whose dimensions are variable.

CHAPTER IV

DETECTION SYSTEMS FOR NEUTRON RADIOGRAPY

The detection systems used in neutron radiography can be classified into two general groups; photgraphic detection systems and non photographic detection systems. Each of these systems will be considered separately.

4.1. Photographic Detection Method

Although, there are a number of available medthods for photographically detecting neutrons, such as special film emulsions loaded with neutron absorber, boron and lithium or normal photographic film, the conventional way is to use x-ray film with a converter screen.

Since neutrons have very little effect on photographic film these converter screens are used to convert the neutron image into alpha, beta or gamma radiation which can be detected more readly by the photographic film.

The photographic detection methods involve two different approaches according to the converter material, given in Table (4.1) which are prompt emission or potentially radioactive materials. The first type of materials are used in direct exposure method in which film and screen are exposed together to the neutron image, the second type is used in the transfer exposure method in which the image is detected first by radioactive converter screen then this screen placed next to the photographic film (see Fig. 4.1)

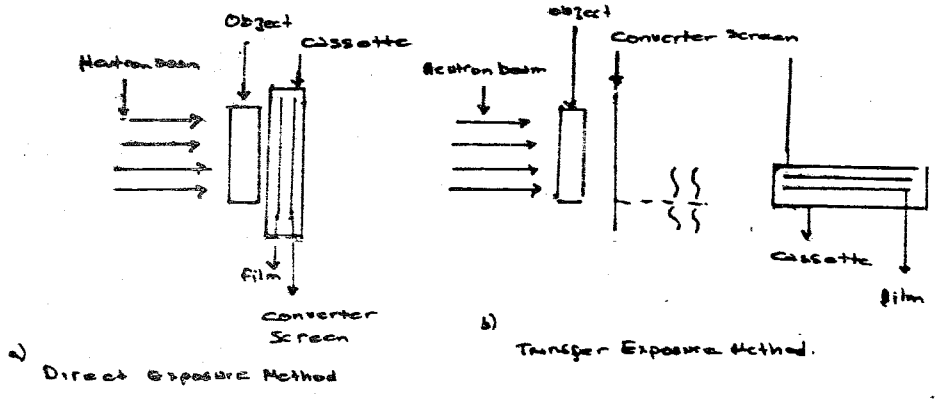

Fig. 4.1. Photographic film exposure methods for neutron radiography.

TABLE 4.1. Characteristics of Several Neutron Photographic Image Intensifier Materials (5).

Material	Isotope Involved Inreaction	Relative natural abundance (%)	Cross section for thermal neutrons (barns)	Reaction	Half-Life s - sec m - min h hours d days	Emission Type	Emission Max Energy Mev
Lithium	Lithium-6	7.52	910	$^{6}Li(n,\alpha)^{3}H$		α	4.7
Boron	Boron-10	18.8	3,770	$^{10}B(n,\alpha)^{7}Li$		α	2.3
Rhodium	Rhodium-103	100	12	$^{103}Rh(n)^{104m}Rh$	4,5 m	β	2.41
			140	$^{103}Rh(n)^{104}Rh$	44 s	x-ray	0.02
Silver	Silver-107	51.35	44	$^{107}Ag(n)^{108}Ag$	2,3 m	β	0.5
	Silver-109	48.65	2.8	$^{109}Ag(n)^{110m}Ag$	270 d	β	1.64
			110	$^{109}Ag(n)^{110}Ag$	24.2s	β	0.43
Cadmium	Cadmium-113	12.26	20.000	$^{113}Cd(n,\ )^{114}Cd$		γ	2.87
Indium	Indium 115	95.77	115	$^{115}In(n)^{116m}In$	54.1m	β	1.5
			52	$^{115}In(n)^{116}In$	13 s	β	0.66
Samarium	Samarium-149	13.8	40.800	$^{149}SM(n,\gamma)^{150}Sm$		γ	9
	Samarium-152	26.8	140	$^{152}Sm(n)^{153}Sm$	47 h	β	3.3
Gadolinium	Gadolinium-155	14.73	61.000	$^{155}Gd(n,\gamma)^{156}Gd$		e	0.44
	Gadolinium-157	15.68	240.000	$^{157}Gd(n,\gamma)^{158}Gd$		e	1.0
Dysprosium	Dysprosium-164	28.1	500	$^{164}Dy(n)^{165}Dy$	1.25 m	β	0.42
			2.000	$^{164}Dy(n)^{165}Dy$	140 m	β	0.8
Gold	Gold-197	100	96	$^{197}Au(n)^{198}Au$	2.7 d	β	0.1

4.1.1. Direct Exposure Method

As already indicated, in this method the film and screen are exposed together to neutron beam, so that the film may be present to detect the prompt radiation emitted from the screen (See Fig. 4.1). The screens which are used in direct exposure method are lithium, boron cadmium, gadolinium, silver and rhodium other materials listed in which become radioactive easily, can be used in the transfer exposure method. (5)

The direct exposure method is a fast detection technique but it has a disadvantage such that: if the beam has high interfering gamma radiation or the radiographed object is radioactive and emits gamma rays, the film present to detect these gamma rays will be gamma-fogged Also radiations which are emitted by reactions between neutrons and the inspected object or with other objects in the beam path present the same problem.

In considering a metarial listed in Table 4.1 for use as a direct exposure converter screen, one must think about what thickness creen to use, the relative speed or resolution which can be obtained with that material compared to others and whether the screen should be pleced on the neutron side of the film (called front screens) or on the back side of the film. (called back screens)

In general, the choice of the converter thickness is a compromise between high resolution and short exposure times. Thick screen leads to a short exposure time but, this time resolution is sacrifised. Berger has worked on to determine the optimum thickness of a particular converter (or intensifier) screen which would produce the greatest film density for a given neutron exposure, by sandwiching x-ray film between known thicknesses converter screen material and exposing this combination to the neutron beam for a known total neutron exposure. Figure (4.2) shows experimental results for Cadmium, which can be used to determine the optimum screen thickness and combination.

It can be seen from Figures 4.2 that the curves all tend to level off for a back screen thickness of 0.020 inch. and that the highst density curve is obtained for a front screen thickness of 0.10 in. Similar considerations from other figures show that the optimum film density,

(best speed for a given converter screen) can be obtained using 10-10 Rh, 20-30 In, 18-18 Ag.0.5-2 Gd[x](5).(14).

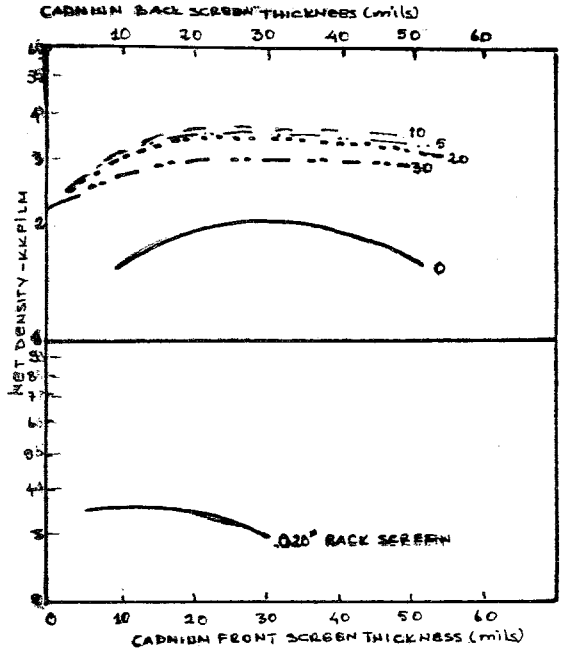

Fig. 4.2. Film density yielded by equal neutron exposures of several double cadmium screen thickness combinations used in direct exposure method (Numbers on curves (upper part) refer to cadmium front screen thikness in mils). Best speed is produced by a 10-20 screen combination (5).

Theoretically the thikness of a converter screen which would produce the greatest film density for a given neutron exposure can be estimated by considering the absorption of neutrons by converter screen and the attenuation of emitted radiation within the screen material. For the beta emitters, such as gadolinium, an estimate of screen thickness can be made on the basis of the range of the emitted beta energy. Borger showed that for the most part, the front screen thickness which yield the best experimental result was in the order expected from the range of the most intense beta energy. For the gamma emitters such as cadmium, the thickness for the optimum density should essentially absorb the neutron beam (5).

---

[x]It is usual to use a short-hand designation such as 10-20 Cd to describe a set of screens having a thickness of 0.10 in. as a front screen and 0.020 in. as back screen.

The relative speed comparisons between different converter screens has been performed by Berger. He used the optimum screen thikness for each converter screen and pointed the relative speed for each of them. The results are summarized in Table 4.2. From Table 4.2 it will be seen that the order of the relative photographic speed for metal direct exposure converter materials in decreasing order, is rhodium, indium, gadolinium and cadmium. This fact has also been confirmed by various workers (14).

It will be noticed that the fastest exposure speed can be obtained by scintillator converter screens. These converter screens consist of a mixture of a neutron absorber and a phosphorous material such as a mixture of Boron-10 and ZnS (Ag) etc.

TABLE 4.2. Relative Photographic Speed of Several Direct Exposure Methods (5).

Converter Material and Screen Configuration (1)	Film Type	Relative Photgraphic Speed
^{6}Li Enriched Santillator as Back Screen (5)	F	50
^{10}B Loaded Santillator as Back Screen (6)	F	35
Rhodium (10) - Gadolinium (2) Screen (7)	KK	1.6
Double Rhodium Screens (10-10)	KK	1.4
Double Gaddinium Screens (1-2)	KK	1.1
Double Indium Screens (20-30)	KK	1.1
Double Dysprosium Screens (3-10)	KK	1.1
Double Cadmium Screens (10-20)	KK	1.0
Double Silver Screens (18-18)	KK	0.8
Single Dysprosium as Back Screen (10)	KK	0.75
Single Gaddinium as Back Screen (1)	KK	0.71
Single Cadmium as Back Screen (10)	KK	0.67
Single Rhodium as Back Screen (10)	KK	0.62
Single Indium as Front Screen (20)	KK	0.5
Single Silver as Front Screen (15)	KK	0.35
Double Gold Screen (6,10) (8)	KK	0.3
Film Only - No Converter	KK	0.03

(1) Numbers in connection with metal screens refer to screen thickness for front screen and back screen, respectively, in mils.

As a scintillator screen, two main types are in use and these are; the mixture of ^{6}Li and $ZnS(Ag)^{7}$ in a matrix of organic plastic material about 4 mm thick and cerium-detivated Lithium glass about 1 mm. Both scintillators are normally made with lithium enriched in ^{6}Li (5). On the other hand boron polyester enriched in ^{10}B has also been used as scintillator screen. In these converters, ^{10}B and ^{6}Li have high cross sections for (n, α) reaction, the resulting α emission causes light emission from the phosphor such as ZnS(Ag), contained in these converters. This method yields faster response than the method in which the alpha radiation is used directly on the film.

The efficiency of ^{6}Li-ZnS(Ag) scintillator screen depends on several factors, these are the ratio of ^{6}Li to ZnS(Ag), the particle size, distribution and thickness. The large granular mixture particles degrade the resolving power of screen and reduce the light output. In addition the ratio of ^{6}Li to ZnS must be constant across the screen and the mixture must be dispersed homogeneously through out the plastic. The light output of ^{6}Li-ZnS(Ag) changes with temperature (15).

Table 4.3 shows some characteristics of scintillators screens

TABLE 4.3. Some Characteristics of Thermal Neutron Intensifiying screens (3)

Screen type	Typical thickness (mm)	Typical neutron registration efficiency (%)	Inherent unsharpness (μm)	Beam n/γ ratio for ~90% n 10%γ image (n-cm^{2} mR^{-1})
421 (granular)	0.65	30	1000	$5x10^{4}$
426 (granular)	0.25	20	400	$5x10^{4}$
905 (glass)	1.0	80	400	$5x10^{5}$

The radiograps obtained by the santillator technique are subject to reciprocity law failure. The same total exposure for a santillator-film detector at one intensity will not necessary produce the same film density, as would be for incal direct exposure neutron radiograph (16).

---

[x] NE stands for Nuclear Enterprise which produces such scintillator detectors.

As has been pointed out before, one should also consider the resolution properties of converter screens. Berger has made some tests using cadmium and gadolinium test objects which contained holes whose spacing varied from very small to large values (See Figure 4.3). The resolution obtained for a converter screen was determined by a number of observed deciding which hole images could still be resolved as separate holes on the radiograph. The result was such that, godalinium-rhodium and ^{10}B loaded scintillators are one which can begin to compare with the sharpness of the transfer radiograph. The poorest sharpness was obtained with cadmium screens. Later studies showed that the best resolution can be obtained by gadolinium screens (5). The resolution capabilities of converters can be explained, by high cross section for thermal neutron absorbtion, a fact which permits the use of very thin screens with reasonable exposure times and the radiation emitted[x]. Since gadolinium has high absorption cross section and emits very soft β radiation (around 70 kev) by means of internal conversion electrons, its use results in the best image sharpness of inspected object (3).

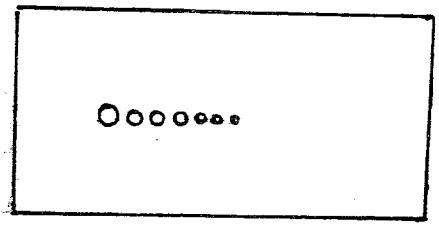

Fig. 4.3 Cadmium resolution test piece.

Although light emitting screens provide much faster results they have a major disadvantage in their poor spatial resolution, because the film exposure is due to light photons rather than the immediate product of neutron absorbtion and produce images which tend to have a grainy apperance due to the grain size of phorophers. Scintillating glasses painted with black light-absorbing paintimproves the resolution to a point where it can compete with foil transfer method buttend to increase exposure time (15).

---

[x]The greater the penetration of the radiation, the power the resolution would be expected because of the increasing tendency for a spread of the image it in the photographic emulsion.

The choice of the screen as back or front screen also effects the speed and resolution. In case of single metal converter screen, the use of front screens yield best speed results except cadmium, which yields about equal response for both front and back screens and gadolinium which yields better speed when used as back screen (17). However some experiments have shown that the use of back screens yields better resolution than the use of front screens (14). On the other hand the use of double metal converter screens on each side of the film yields faster results than the use of single converter screen but resolution will be decrease. From Table (4.4) one can see various converter screen which have optimum screen thickness and orientation for good resolution characteristics. In this table a compromise converter screen thikness between speedand resolution had beed used for the single matel screen materials.

It is interesting to note that the use of double cadmium screen increases the film density, although 0.010 in front cadmium screen absorbs about 95 percent of the neutron beam. The additional density produced by the back screen is due to electron emission and secondary radiation general in cadmium by the hard gamma radiation of the (n,γ) reaction in cadmium.

In direct exposure method, another important fact is the relative response of the detector to neutrons and gammas. This relative response is determined by the thermal neutrons/cm^2 required to produce the same film density when detector is exposed to one miliroentgen of ^{60}Co gamma radiation, and is usually measured by neutron to gamma response ratio (neutrons/cm^2 per milliroentgen). Berger has showed that the smallest response can be obtained by using scintillator -film direct exposure method (5),(14).

The importance of these response ratios will appear when inspection problem is such that the relative absorption of materials for neutrons is quite different from that of gamma radiation. For example if one were inspecting boron steel samples to determine the uniformity of boron distribution, the neutrons would yield a potentially high contrast image because of the high neutron attenuation of boron and lower attenuation in steel, this contrast would be reduced if the detector system also responded to gamma radiation, because of the reversed attenuation characteristic of gamma radiation. This problem can be avoided by transfer exposure technique.

TABLE 4.4. Neutron Image Resolution Summary of Direct Exposure Methods

Converter Screen Material Thickness and Orientation	Cadmium Test Piece	Gadolinium Test Piece	Screen Thickness Investigated (mils)	Neutron Exposure Time for AA Film Density of 1.5 (min)	Remarks
0.5 Gd, back	1,2 mils	0,4 mils	0.25 to 2	11.1	
3 Cd, back	1,2	-	1 to 30	15,1	
3 Rh, back	2	-	3 to 10	17.1	Single metal screen exposure methods
5 In, front	2	-	2 to 30	23	
10 Dy, back	2	-	5 to 10	8.1	
5 Ag, front	2 to 3,6	-	5 to 30	21.75	
^{6}LiF powder, back	1.2	1.0	60	25	Compressed ^{6}LiF powder, 95.6% enriched
^{6}Li, ZnS(Ag)	2	-	8	0.1 (Tri-X Film)	Modified Stedman type scintillator 96%^{6}Li enriched (6)
^{6}Li, ZnS(Ag)	2	-	60	0.1 (Tri-X Film)	1:4 powder mixture (7) using 96% enriched ^{6}LiF and ZnS (Ag)
^{6}Li Loaded Glass	2	-	75	1	Cerium activated silicate glass containing 2.5% Li, 96% enriched with ^{6}Li
^{10}B, ZnS (Ag)	2	-	12	1	Sun type scintillator (9), 92% enriched with ^{10}B
10-10 Rh	2 to 3.6	-	3 to 10	4.3	
20-30 In	3.6	-	2 to 30	5.5	Double metal screen methods
18-18 Ag	3.6	-	5 to 30	7.5	
10-20 Cd	20	-	1 to 30	6	
0.25-2 Gd	1.2	0.4 to 0.7	0.25 to 2	4.8	Fastest double Gd technique
10 Rh-2 Gd	1.2	1 to 3	10 Rh-2 Gd	3.85	Fastest metal screen method

4.1.2. Transfer Exposure Method

As has been pointed out previously, the use of potentially radioactive metal converter screen in the transfer exposure method eliminate the effect on the film of any other radiation in the neutron beam. However this transfer method, also yields radiographs having better resolution than the direct exposure methods. This is partly due to scatter in the film emulsion and backing material during direct exposure and partly due to elimination of hard gamma radiation from (n,γ) reaction in the transfer method[x]. The disadvantage of this technique is that it requires long exposur time.

For transfer screen material it is required that screen material should have high activation cross section and produce an isotope with a convenient half-life, long enough for food statistics in stored image and short enough for convenient read out on to film and thence re-use. For example, silver and rhodium is not in generally useful as the other materials, because of their short-half lives, saturation activities are quickly reached and most of radiactive nuclei decays before enough build-up of radioactive nuclei is attained to expose the film.

To understand the point indicated above, it will be useful to look at the build-up activation of the detection materials when exposed to the neutron beam. The activity produced, A, can be found as follows

$$\frac{dN(t)}{dt} = \Sigma a\phi - N(t)\lambda \tag{4.1}$$

$$N(t) = \frac{\Sigma a\phi\ (1-e^{-\lambda t})}{\lambda} \Rightarrow\ A = \Sigma a \phi\ (1-e^{-\lambda t}) \tag{4.2}$$

---

[x]It will be seen from Table 4.1 that transfer converter screens have beta activity.

Where

A is the activity produced (desintegration/sec)
Σa is total activation cross section of converter material
λ is the decay constant
ϕ is the thermal flux at the surface of converter screen
t is the irradiation time
N(t) is the number of radioactive nuclei produced.

Note that the activity produced is directly proportional to the magnitude of the flux at the surface of the converter screen and if the exposure time increases, the saturation effect is reached. i.e. the activity will be equal to production rate. Also it will be seen from equation (4.2) that there is little to be gained in exposing a given material to a given neutron flux for exposure times beyond several half lifes. The same fact is valid when the transfer screen material has been transferred to a film for decay.

The materials which are mostly used as transfer detection screens were given in Table (4.1). From these materials dysporsium, samarium, indium and gold appear to be the most useful.

Except for relative neutron-gamma response the same characteristics involved in the direct exposure methods are also valid for the transfer method.

Berger has reported that, using an identical neutron exposure and transfer time for a given screen material, there would be little gained in the film density by using indium screen thicker than about 0.020 in. dyspersium thicker than 0.01 in or gold thicker than 0.005 in. He has also showed that these optimum screen thickneses are sufficiently thin so that both sides of the screen become almost equally active (5).

The resolution properties of these converter screens are given in Table (4.4). From Table (4.4) one can see that the best resolution can be obtained by using gold and the best speed can be obtained by using dysporsium.

TABLE 4.5. Neutron Image Resolution Summery of Some Transfer Exposure Methods (3).

Converter Screen Material and Thickness	Cadmium Test piece	Gaddinium Test piece	Screen Thikness (mils)	Neutron Exposure Time for A.A. Film Den of 1.5 /min
3 Ay	1.2	1.0	3 to 10	240
2 In	2	--	2 to 30	163
10 Dy	2	--	5 to 10	14.6

Another property which must be considered for transfer converter screens is the ability to produce radiographs with low intensity beams not only with non-reactor neutron sources but also in reactor work, with highly absorbing objects. Thus it is necessary to estimate the minimum beam intensity for image production for given metal foil thickness. As an example consider a 100 μm dysprosium which produces good radiograph with a thermal dose of 10^7 n/cm^2/sec.

$$A \propto \phi(1-e^{-\lambda t})$$

where A is the activity produced

ϕ is the thermal flux level

t is irradiation time

λ is the decay constant - 5×10^{-3} min.

Assuming a maximum integration time for dysporsium screen of three half lifes which is equal to eight hours.

The radiaton dose impartted to the film is given by

$$D \propto \int_0^{\infty} Ae^{-\lambda t} = \frac{A}{\lambda}$$

So that the dose is determined by the activity as long as dysprosium is allowed to decay completely i.e. for eight hours.

TABLE 4.6. Minimum Beam Intensities for Radiography Using the Transfer Technique (3)

Screen Metal	Activation cross-section mm^{-1}	Absorbtion in 100 m screen (%)	(s^{-1})	10^3s	Minimum Thermal beam Intensity For exposure times of (cm^2sc^{-1}) 104	10^5	Activity after 10^3s in beam of 10^7 $cm^{-2}s^{-1}$($cicm^{-2}$)
In	0.73	7.3	$2.114x10^{-4}$	$4x10^5$	$9x10^4$	$8x10^4$	4.2
Dy	3.01	2.6	$8.25x10^{-5}$	10^5	$2x10^4$	$8x10^3$	5.8
Au	0.58	5.6	$2.98x10^{-6}$	$5x10^5$	$5x10^5$	$6x10^2$	0.05
Eu	8.90	5.9	$2.09x10^{-5}$	$4x10^4$	$4x10^4$	10^3	3.3

[x]Although the best speed can be obtained with Eu, it is not stable in air (3)

Since A is known from current experience, for a flux of 10^7 n cm^{-2}-S^{-1} (18), the irradiation time is 1 min, the lowest value of flux with which transfer radiography is possible can be found by

$$\phi(1-e^{-\infty}) = 10^7(1-e^{(-5x10^{-3}x1)})$$

$$\phi = 5x10^4 \text{ n } cm^{-2} sec^{-1}$$

Until now we have been concerned with the properties of interest for photographic detectors in thermal neutron radiography similar detection techniques can be applied for epithermal and fast neutrons. The materials which are useful in the epithermal or resonance neutron energy region are given in Table 4.6. These materials can be used as converter screens for either the direct exposure or transfer exposure methods.

TABLE 4.7. Useful Detectors for Epithermal Neutrons (1).

MATERIAL	ENERGY OF MAIN RESONANCE	ISOTOPE INVOLVED	HALF-LIFE PRODUCED
Indium	1.46 ev	^{115}In	54 min
Gold	4.9 ev	^{197}Au	2.7 min
Tungusten	18.8 ev	^{186}W	24 hours
Lanthanum	73.5 ev	^{139}La	40 hours
Manganese	337 ev	^{55}Mn	2.56 hours

4.2. Nonphotographic Detection Methods

4.2.1. Track-Etch Image Recorders

When energetic ions pass through dielectric materials such as mica, glass and plastic, they leave tracks of damage in their wake. This track formation can be explained by the fact that when a charged particle passes though material, it produces ionization along its path. Then these ions repel each other so that a narrow cavity surrounded by a region under high strain produced in crystalline structures or ionization produces broken chains and frees radicals. In both cases the resulting region is chemically highly reactive because of highstrain.

Although the latent image tracks can be seen under the high magnification of an electron microscope, it is conventional to use chemical etch to reveal a visual image of tracks (19).

Detection of thermal neutrons is done by using a suitable combination of charged particle producing screens in contact with sensitive dielectric material (solid state track detector, SSTD). Screens of fissile materials, alpha producing elements such as L_i and Bo can be used succesfully. However, the cost, poor stability of fissille material, ^{235}U, in air and radiographic back ground due to its natural α activity lead to interest in screens emitting α particles. The suitable α emitting screens are their fluoride and carbide, i.e. LiF and B_4C (3).

The principle of neutron radiography using SSTDs[x] is the same as for the conventional radiographic methods except that a charged particle sensitive SSTD is used instead of conventional photosensitive film.

The most useful SSTDS are polycabonate plastic, which has greater sensitivity to fission fragment, and cellulose nitrate, which has greater sensitivity to radiation. Their etchanst is 6.5 N.NaoH. However , mica and glass plates are etched in HF acid which requires careful handling.

The advantages of track etch technique over conventional photographich detection techniques are:

a) They are cheap and versatile

b) Their registration efficiency is essentially unimpaired by large back grounds of β's, γ's and neutrons therefore provide good image detection for radioactive materials.

c) It has no light sensitivity which allows ease of handling and track development can take place in daylight and can be arrested for inspection and restarted.

d) It provides better resolution than transfer technique

e) It provides infinite image accumulation time.

[x] SSTD'stands for Solid state Track etch Detector

The disadvantages of this method are that ^{235}U screen produce high alpha background when used in combination with cellulose nitrate detector and low contrast in images. However it is possible to enhance image contrast by some methods such as, contact printing, scattered light anlargement, the use of fluorescent material and polarized light and red dyed plastic films (2

Table 4.7 shows some of the most commonly used solid state track detectors and their suppliers.

TABLE 4. . Etching Conditions for Some Commonly Used Solid State Track Detectors(20).

Detector	Suppliers	Etching Condition
Daicel	Dia Nippon Co., Japan	6.25 N naOH, 10 min., 55°C
		28% KOH, 30 min., 23°C
LR 115	Kodak Pathé, France	25% NaOH, 10 min., 55°C
Makrofol	Bayer, A.G., Leverkusen	6.25 N NaOH-4% Benax
	W.Germany	20 min, 55°C
T Celit	Bayer, A.G., Leverkusen	18% NaOH, 14% KOH, 3.6%KmnO4
	W. Germany	and 64.4% H_2O, 20 min 55°C
		Q 25% KOH, 25 min, 60°C
Traifol	Bayer, A.G., Leverkusen	25% KOH, 2 hours, 60°C
	W. Germany	
Lexan	General Electric, Pitts	6.25 N NaOH-4% Benax
	Pittsburg Pa., USA	20 min, 55°C
Soda Lime Glass	"	
Muscovite Mica	"	
Biotite Mica	"	

4.2.2. Electronic Image Recorders

The major disadvantage of image recorders of photographic type is to give immediate image presentation, although the use of polaroid film can largely over come this fact. However, electronic method of immediate image presentetion may also be used, but they are incomparably more expensive than the screen film method. Before considering electronic image presentation it will be useful to consider fluoroscopic image detection method because it is the basis for electronic image presentation.

Fluoroscopic image detection is used for production of visible image on a fluorescent screen i.e for viewing the fluoresecent image with dark adapted eyes during the examination of inspected object. These screens are generally made of zinc sulfide or cadmium sulfide cryslals or mixture of LiF in case of neutron image method. The natural spectral emission of these screens can be charged by the manufacturer to suit certain applications by adding minute amounts of impurties, sc called activatòrs. For example the use of Cu activator with zine cadmium sulfide produces green colour light which match closely the spectral sensitivity of the humen eye.

Rather than directly viewing the fluoroscopic screen, the radiation shielding problem in such a detection arrangement would be eased with the use of a closed circuit televion system to bring the fluoroscopic image out of radiation area. With most radiography units the neutron beam stregth is too low to give sufficient light intensity to be seen in monitor so image intensifiers are placed between the fluoroscopic screen and the camer

Berger has developed a thermal neutron sensitive version of a x-ray image ntensifies in which the radiation sensitive material is LİF ZnS (3).

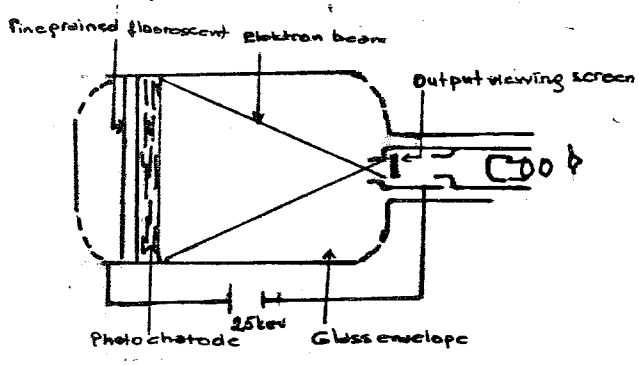

Fig. 4.4. An image amplifier system

An image amplifier system consists of a highly evacuated glass tube at one end of which is a larger of fluoreserent material called the input phosphor, coating the interiors of the tube (see Fig. 4.4) A photo emissive layer consisting of a compound of, e.g. cesium, antimony is placed adjacent to input phosphor and acts as a photochatode. This photo emissive layer emits low energy electrons when exposed to the light of the fluorescent screen. Hence the fluorescent screen image is converted into an electron

image. The electrons are accelerated by a potential about 25 kV and brought upon a phosphor screen at the viewing end of tube which is fine grained and has a smaller size than the input screen. The output image is many times brighter than the one formed on the large screen. This is due to the increase of energy acquiredby the electrons and the reduction of fluorescent image. Hence the image need'nt be viewed in the dark and can be seen on a TV monitor because of its high brightness level (21).

In case of x-ray image intensifier of this type, the electrons image within the intensifier tube is obtained by the process x-ray-light electrons however in the case of neutron image intensifies the process is neutron-alpha-light-electrons.

Although inherent sharpness is comparable with NE 421 film, situation when the same screen is used, geometric unsharpness will be poor since screen is some what inside the front of the tube. Chalmeton has developed a new neutron sensitive intensifier in whichgadolinium was used in place of the usual photochatode and placed it very near the surface of the vacuum envelope. In this case spatial resolution and neutron registration efficiency will be somewhat higher (3).

A more straight forward approach is to use modern high gain image intensifier TV camera assembly to view the back face of a light emithing screen through a fast lense and a 45° miror.

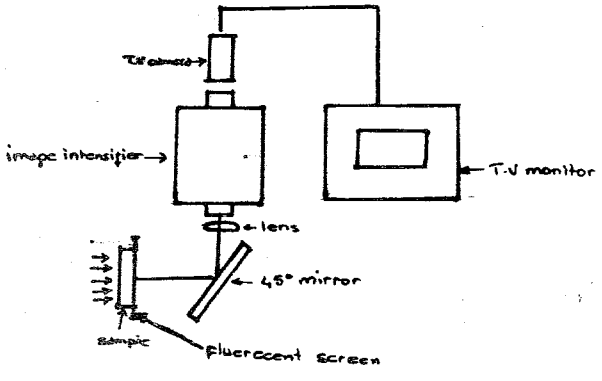

Fig. 4.5. Television system for neutron radiograhy.

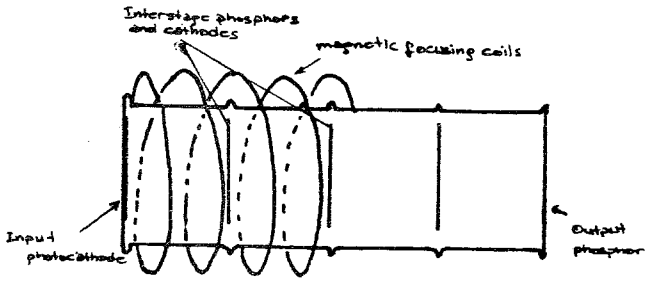

Fig. 4.6. The diagram of the thermal neutron image intensifier (Cascade Type) (22).

The high gain image intensifier is of the cascade type as shown in the Figure 4.6. The photo electrons produced at the input photoemissive layer are acelerated several kilovolts and focused on the first dynode with an multiplying factor, and electrons released from the last dynode are accelerated onto a phosphore screen while maintaining then spatial position by means of magnetic focussing coils (22).

Most intensifiers are compatible with a standard vidiocon tube and a number have a photochade sensitivity which is a good spectral match with the ZnS(Ag) phosphor.

With these systems the thermal neutron intensities as low as 10^5 n/cm^2-see is required for useful image. However Berger has shown that the thermal neutron intensities as low as 10^3 n/cm^2-sec could be detected by means of a closed circuit orthicon television system. However in this case because of statistical variations, some integrating technique such as a storage tube output, a slow scan television technique, or simply photography of television presentation can be used (3), (21).

As well as immediate image presentation electronic image recorders provide dynamic image presentation i.e. radiography of moving objects, and enable complex objects to be precisely aligned for long film exposure. Therefore, one can, for example observe the motion of light objects in a appreciable thickness of heavy materials. In addition the relatively low responce of neutron image system to high energy gamma radiation permits the neutron examination of radioactive objects.

CHAPTER V

IMAGE SYSTEM CHARACTERISTICS

In neutron radiography, one must have a detailed knowledge about the density exposure curve, neutron registration efficiency, and resolving power in order to make an informed choice of imaging system for a radiographic task. Since the most popular image system consist of a screen film combination, our considerations will be concentrated on this system, however, the underlying principles apply equally well to other systems.

5.1. Density Exposure Characteristics and Spatial Resolution

When protons or electrons fall on to a film emulsion, which is standart x-ray film, electrons and positive silver ions migrate to points of imperfection in the silver-halide crystals, and on arrival some silver ions are reduced to metallic silver to form the latent image. After development with suitable agents the silver halide at the latent image is further reduced metallic silver, and the uneffected halide grains are subsequently dissolved away by the fixing solution, leaving a black metallic silver image. The speed of a film is a mesure of the blackening produced by a given exposure. The greater the grain size, the greater the speed of a film will be. But on the other hand larger grain size means poorer resolution (10).

The signal or degree of blackening of the film, is conventionally referred to as optical density, D, defined as

$$D = \log \left(\frac{I}{T}\right)$$

where I is the intensity of the incident viewing light and T is the intensity of transmitted light.

The characteristic curve is obtained by plotting the density versus total exposure, which is equal to the product of intensity, ϕ, at the image point of interest and exposure time T, $E = \phi T$. Two typical density-exposure characteristic curves for various screen-film combinations are shown in the Figs. 5.1, 5.2.

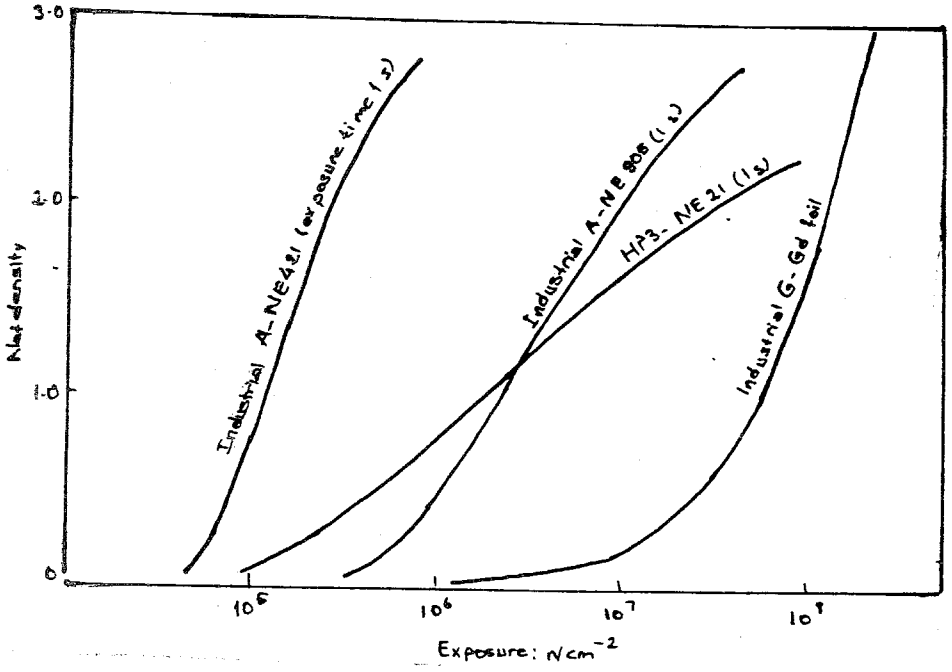

Fig. 5.1. Typical exposure characteristic curves for light-emitting (NE 421 and NE 905-1.3mm) and electron emitting (gadolinium foil 0.025mm) intensifying screens for direct technique thermal neutron radiography used singly behind selected films (24).

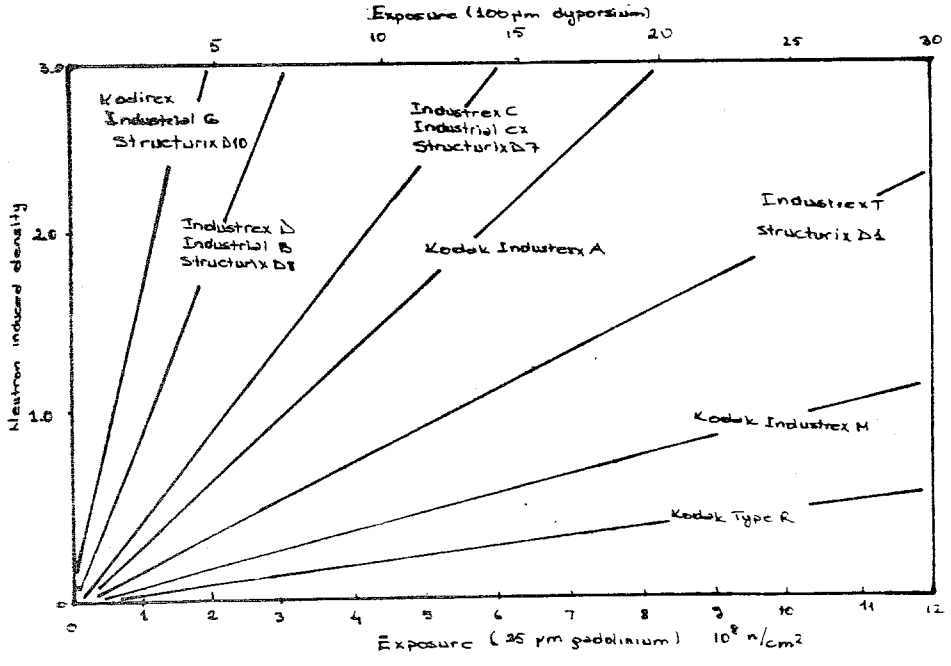

Fig. 5.2. Typical-density exposure characteristic curves for electron emitting intensifying screens of gadolinium and dysporsium(24).

The prediction of exposure necessary to achieve a desired density to better than ± 25 percent should not be expected from such curves. This is due to the nature of the film which makes it impossible for a manufacturer to market a precisely characterized product, and the screen response is not constant because the energy spectrum of neutron beam varies from one facility to another (3).

The important points in a signal exposure curve are, the minimum dicernible density, the gradient of density curve, the minimum recognise-able change in density, and the maximum density.

The minimum density which can be observed above background noise is usually termed the threshold in radiography, and the corresponding exposure is termed the threshold speed. The gradient, $G = dD/dE$, is referred to as the contrast of the recorder. The stepper the slope of the curve, the greater will be the density difference. If the film is exposed to light, as in the case of scintillator converter, it is useful to plot the density against the logaritm of exposure because a considerable portion of the curve reveals a straight light in most important range of image densities. The minimum density change, ΔD_{min}, that can be reliably observed is, together with the contrast, the parameter which determines the minimum variation in object thickness discernible on a radiograph.

Consider the simple object of thickness containing a defect of thickness y and let the difference in attenuation coefficients between the bulk object and detail be $\Sigma = \Sigma_b - \Sigma_d$, see Figure 5.3.

The change in the exposure due to y can be found as follows. The neutron flux at the converter screen from two parts of sample would be.

$$\phi_1 = \phi_o e^{-\Sigma_b x} \tag{5.1}$$

$$\phi_2 = \phi_o e^{-(\Sigma_b x - \Sigma_d y)} \tag{5.2}$$

Neglecting the possible differences introduced by scattering process, the flux difference recorded by converter screen will be:

$$\Delta\phi = \phi_2 - \phi_1 = \phi_o (e^{-(\Sigma_b x_1 + \Sigma_d y)} - e^{-\Sigma_b x}) \tag{5.3}$$

$$x_1 = x - y$$

$$\Delta\phi = \phi_o \; e^{-\Sigma_b x} \; (e^{(\Sigma_b - \Sigma_d)y} - 1) \cong \phi_o \; e^{-\Sigma_b x} \; (e^{\Sigma y} - 1) \tag{5.4}$$

$$\Delta\phi \quad \phi_o \, e^{-\Sigma_b x} ((1 + \Sigma y - \ldots) - 1)$$

$$\Delta\phi = \phi_o \, e^{-\Sigma_b x} \Sigma y \tag{5.5}$$

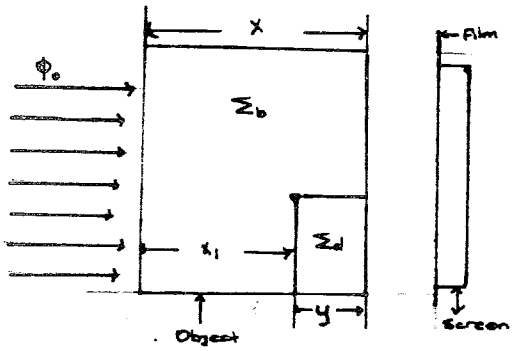

Fig. 5.3. A schematic drawing image detection.

Since $E = \phi t$ and taking the bulk exposure as $E = Ioe^{-\Sigma_b x}$. The exposure difference will be

$$\Delta E = E\Sigma dy \tag{5.6}$$

which will give rise to a density change

$$\Delta D = E\Sigma y \frac{dD}{dE} \tag{5.7}$$

Then the minimum detail thickness that can be discernible, is

$$y_{min} = \frac{\Delta D_{min}}{E\Sigma \frac{dD}{dE}} \tag{5.8}$$

If the characteristic curve is plotted in the usual logarithmic exposure scale the curve is linear over the range of densities used in most radiographs, turns out to be 0.5 to 2.5. Then the equation describing this line is

$$D = G \log E \quad \text{Constant}$$

Therefore

$$\frac{dD}{dE} = 0.434\ G\ \frac{dE}{E} \tag{5.9}$$

Substituting this value in Eq (5.8) the thickness sensitivity will be

$$y_{min} = \frac{2.3\ \Delta D_{min}}{G\ \Sigma} \tag{5.10}$$

In the case of linear exposure scale, such as for β emitting screens, the characteristics curve is linear, see Fig. 5.2, therefore the density will be

$$D = GE + \text{Constant}$$

Hence, with equation (5.8)

$$y_{min} = \frac{\Delta D_{min}}{G \Sigma E} \tag{5.11}$$

From equations(5.10) and (5.11) one can see that the sensititity improves when exposure is increased. However, this relation is only accurate when low gamma ratio beams are used in radiography of objects producing little secondary radiation because γ ray background presents problem during the exposure.

In the presence of gamma background the fractional sensitivity $C = y_{min}/x$, is more useful measure of radiographic performance. Then with Eq. (5.10)

$$C = \frac{2.3\ \Delta D_{min}}{G \Sigma x} \left(\frac{E + B}{E} \right) \tag{5.12}$$

where B is the exposure due to background radiation.

When the recorder response is linear with exposure, background radiation has no effect on sensitivity, beyond adding a constant amount

all densities.

The thickness sensitivity for a variety of material have been measured in the range 1-10 percent. The sensitivity can be increased for objects in which only parts of interest is highly neutron absorbant. (3).

The spatial resolution detectable in neutron radiography can be described quantitavely in terms screen-film unsharpness (inherent unsharpness) and geometric unsharpness.

In neutron radiography, the presence of converter-screen as an intermediate state introduces unsharpness due to the radiation emitted by the screen which has a great angular spread and enter the film obliquely at some small lateral distance from its origin in the screen. The value of screen-film unsharpness depends on the range of emitted radiation, the thickness of converter screen and type of the film.

The screen-film unsharpness can be obtained, as a single figure, by measuring the density change as a function of distance accross the image in a number of ways. The most popular of them is the Klasen's method in which a knife edge object is placed in contact with the image recorder, thus eliminating geometric unsharpness, and the value obtained for unsharpness is only due to the screen-film unsharpness. This method of unsharpness determination is shown in the Figure 5.4.

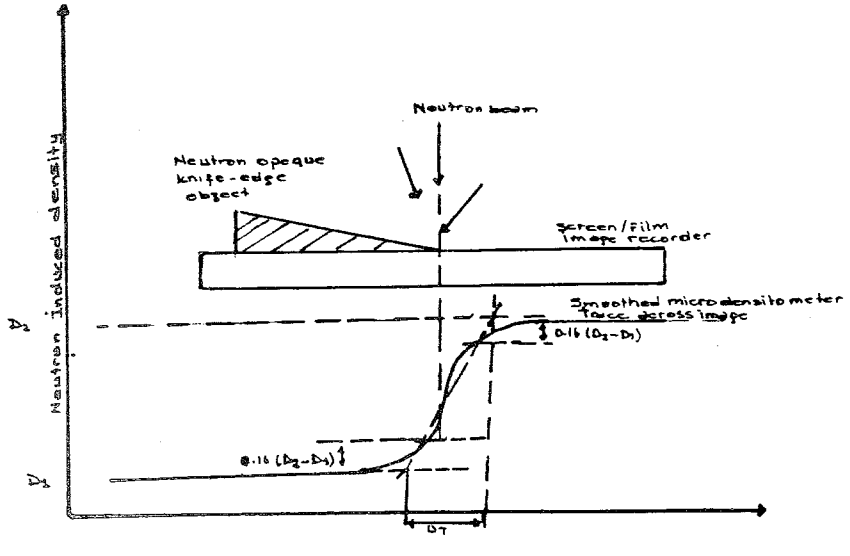

Fig. 5.4. Illustration of Klasens's method for measuring the unsharpness of film-screen combination (10).

The number obtained this way is a characteristic of the recorder system and this is also termed as inherent unsharpness which together with geometric unshaprness, is a measure of the smallest descernible detail.

However, the figure obtained this way presents problems because knife edge image traces with same unsharpness numerically may not necessarily have the same basic shape and give the resolution at one particular contrast value. The eye is peculiarly sensitive to some forms of density change which are then interpreted as differences in resolution.

The failure of this system is such that it does not allow the radiographer to evaluate the system design and fine tune to produce maximum information in radiography. Hence in recent years radiographers developed some complete methods of describing resolving power. One of them is modulation transfer function which is a plot of the fractional response of recorde to contrast variations in the object as a function of the seperation or spatial frequency of the variations. Any image can be expressed as a series of sine waves of differing frequency, amplitude, and phase by the use of Fourier analysis. Therefore a test object which will produce a sinusoidally density variation with known frequency and amplitude provides a means of evaluating the resolving power of radiographic system. Such a test object is shown in Figure(5.5) and an ideal radiographic system should produce an image of such an object without loss or change in information.

Since such test objects are difficult to produce, in neutron radiography the resolving power is obtained by use of a sharpe edge or a narrow slit. The density curve of such system is analys ed into its component of sine waves, and the curves are reproduced as shown in the Figure 5.6.

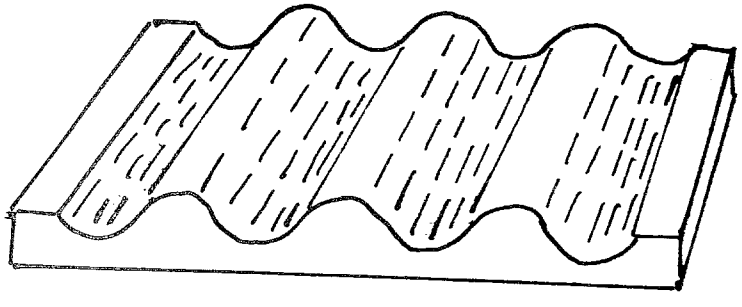

Fig. 5.5. Diagram of a test object whose transmission varies sinusoidally along its length (10).

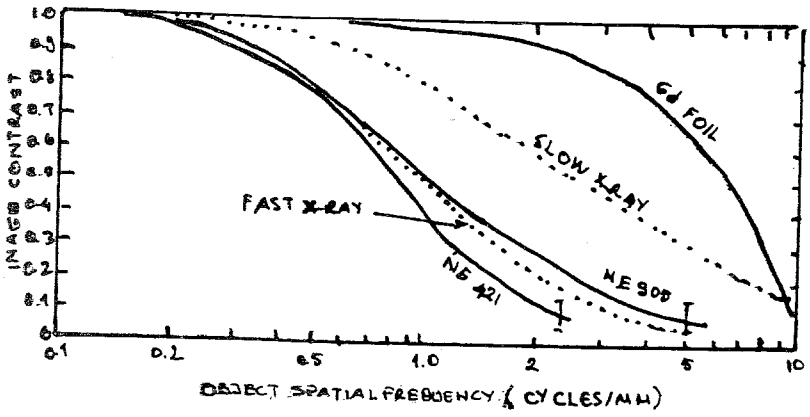

Fig. 5.6. Contrast transfer functions of NE 241 and NE 905 scintillators Gadolinium screen and X-ray films (10).

The resolving power of image system is expressed as the object spatial frequency which can be regarded the maximum number of lines per milimeter that can be resolved from the Figure 5.6 one can see that, with gadolinium screen a sharper radiograph than x-radiograph is obtained.

To obtain an estimate of the size of the smallest detail that can be detected on a radiograph of an object the geometric and inherent unsharpness values must be combined. The figure obtained will determine the size of detail that is descernible. Klasen's suggested the following form of empirical formula

$$U_T = (U_g^3 + U_i^3)^{1/3}$$

where U_T total unsharpness

U_i inherent unsharpness

U_g geometric unsharpness

It must be stated here that this is one of the several empirical formula from the above formula it will be readly seen that use of poor geometric unsharpness with a high resolution recorder will be wasteful in terms of exposure time and neutrons. The optimum situation is one in which U_g and U_i are approximately equal (23), (24).

The smallest detail in neutron radiography is limited ultimately by 'quantum motle', which is the term given to inhomogenitics in images caused by natural statistical fluctuations in the number of particles recorded and in their effect.

In neutron radiography, sometimes low intensity neutron beams must be used and some of intensifying screen may be so effective that fewer than 100 neutron may produce a visible change in the image and this change can be discerned when it shows above natural fluctuations in its surroundings. Hawkes-worth and following workers have shown that two requirement must be fullfilled to detect a void of cylindrical form.

a) The density change between the image of the defect and the surrounding film density must be visible.
b) There must be a sufficient number of particles recorded by the film to ensure that the density of void can be clearly distinguished from density variations due to noise in the region of film surrounding the image of the world where noise is due to the signal and the overall exposure plus background. For a reliable observation of a signal

$$r > k/(R+B)^{1/2}$$

where the confidence factor, k, is the number of times the signal must be greater or less than the standard deviation in similar areas of its surrounding. The value of k varies with application. For example the detection of 1 cm^2 detail in 10 cm^2 object will require a value of k much smaller that for the detection of 1 mm^2 detail in a 100 cm^2 object. (24).

If we consider the detail area, a, and the thickness x as shown in the Figure 5.7 in the absence of image unsharphess this area will give rise to a variation ΔE in the average exposure, E, at the recorder. Assuming that the neutron registration efficiency is η, the debil will give rise to a variation $a.\Delta E\eta$ in the number of neutrons recorded in the area $(a \quad \Delta a)$ with its unsharpness. As already was indicated above this change must be k times greater than the standard deviation in the average number of neutrons recorded in all areas $(a+\Delta a)$. Therefore for a reliable recognition.

$$|a\ \Delta E\eta x| \geq |k((a+\Delta a)E\eta)^{1/2}| \qquad (5.12)$$

If the small detail has an attenuation difference Σ from the bulk object $\Delta E \quad E\Sigma x$, substituting in equation 5.12.

$$E \geq \frac{k^2(a+\Delta a)}{\Sigma^2 \eta a^2 x^2} \tag{5.13}$$

For the recognition of cylindrical detail of diameter x,

$$E \geq \frac{4k^2 (x+u)^2}{\Pi\Sigma^2 \eta x^6} \tag{5.14}$$

This expression makes an estimate of the exposure necessary to recognise a particular detail.

Expressing equation 5.14 in a more appropriate form

$$E = \frac{4k^2}{\Pi\Sigma^2 x^b \eta} \quad ((L_f + \frac{D}{L})^3 + U_i^3)^{1/3} + x)^2 \tag{5.15}$$

$$x^6 = \frac{4k^2}{\Pi\Sigma^2 \eta E} \quad (((L_f + \frac{D}{Ls})^3 + U_i^3)^{1/3} + x^2)^2 \tag{5.16}$$

Relating the exposure to attenuated neutron flux at the screen as

$$E = \phi_o BT$$

where ϕ_o is the neutron flux at the object and B is the fraction of neutrons that are transmitted. Inserting the values of E in to Eq (5.16)

$$x^6 = \frac{4k^2}{\Gamma\Sigma^2 \eta T \phi_o B} \quad (((L_f + \frac{D}{Ls})^3 + U_i^3)^{1/3} + x^2)^2 \tag{5.17}$$

is obtained.

Using the appropriate values this equation is used as the basis for the design of a new facility and several values of D/L can be tried in order to determine the sensitivity of x to this term.

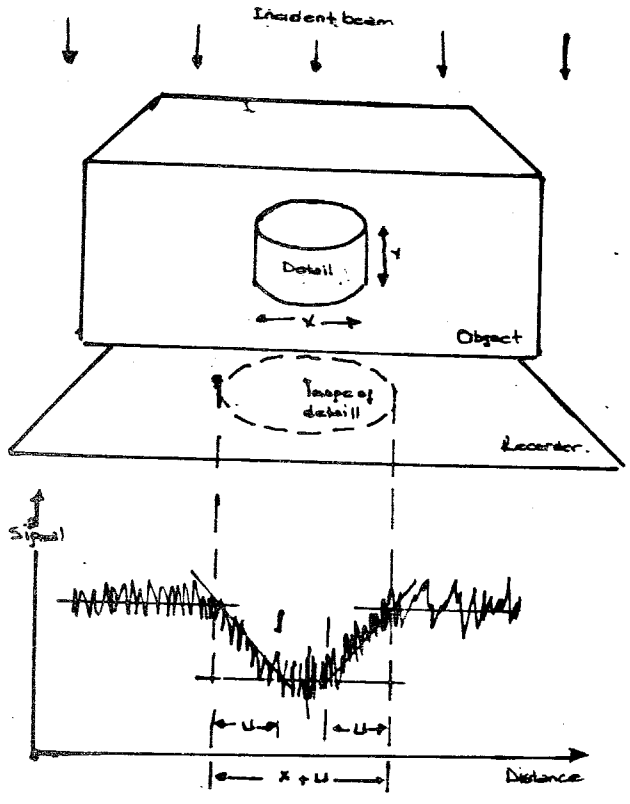

Fig. 5.7. Diagramatic representation of the formation of the image, diameter (x + a) of detail (24).

5.2. Film Types and Processing

Photographic films used in neutron radiography are normal industrial x-ray films. Film producing companies supply a full range of industrial x-ray films from Ultra-fine-grain to high-speed making it possible to choose the right film for any industrial radiography job.

A comparative list of some of photographic films that have been used for neutron radiography are given in Table 5.1.

To produce satisfactory radiographs care must be taken in processing films. The most careful radiographic techniques can be nullified by incorrect dark room procedures. Film processing procedure is accomplished by development, agitation, stop bath or rinse fixing, fixer neutralising, washing and drying.

TABLE 5.1. Approximate Comparison of European and U.S.A. Films (10).

Type	Kodak Ltd. (U.K.)	Ilford Ltd. (U.K.)	Kodak Pathe (France)	Gevaert Agfa N.V. (Belgium)	Estman Kodak Ltd. (U.S.A.)	Du Pont (U.S.A.)	Ansco (U.S.A.)	Ref Speed
	Royal Blue	Gold Seal		Curi x PPL	Royal Blue Type F			
	Blue Brand	Fed Seal		Curi x RP2	Blue Bland	Type 508		
	Indushex S	Industrial A		Structurix-S		Type 504		
	Standard	Standard		Osray T4	Non-screen Medical			
		Ilfex						
		Industrial 6						
	Kodirex				Type F			0.2
			Kodirex	Structurix-B10		Type C		0.3
	Industriex D	Industrial B						0.5
			Analyse					0.6
	Crystallex	Industrial CX		Structurix-D7	Type AA	Type 504	Type A	1
			Deginex					1.2
						Type 506		1.4
		Industrial C						1.5
					Type 7		Type B	2
		Industrial F						3.1
				Structurix-D4	Type M	Type 510		3.8
	Microtex							4
			Type M					5
					Type R			8
				Structurix-D2				15

The list above is arranged in approximate order of speed (fast at the to p)

Each of these steps must be performed according to manufacturer recommendations.

The processed film can be viewed by irect viewing, optical protection, Photographic method, microscopes, and micro densitometer scaning.

5.3. Image Quality Indicators

After neutron radiography has taken its place as a nondestructive test method commercially, methods of measuring image quality and standartization have become essential. One of most widely used image quality indicator is that developed by ASTM (American Society for Testing Material). This image quality indicator,(IQI),consists of two basic parts: beam purity indicator and a sensitivity indicator.

The beam purity indicator consists of a small black of boron nitride 0.315 m thick. The block consists of three holes one containing a thin filter of boron nitride, one containing a boron nitride filter backed by a lead filter and one hole remaining open, see Fig. 5.8.

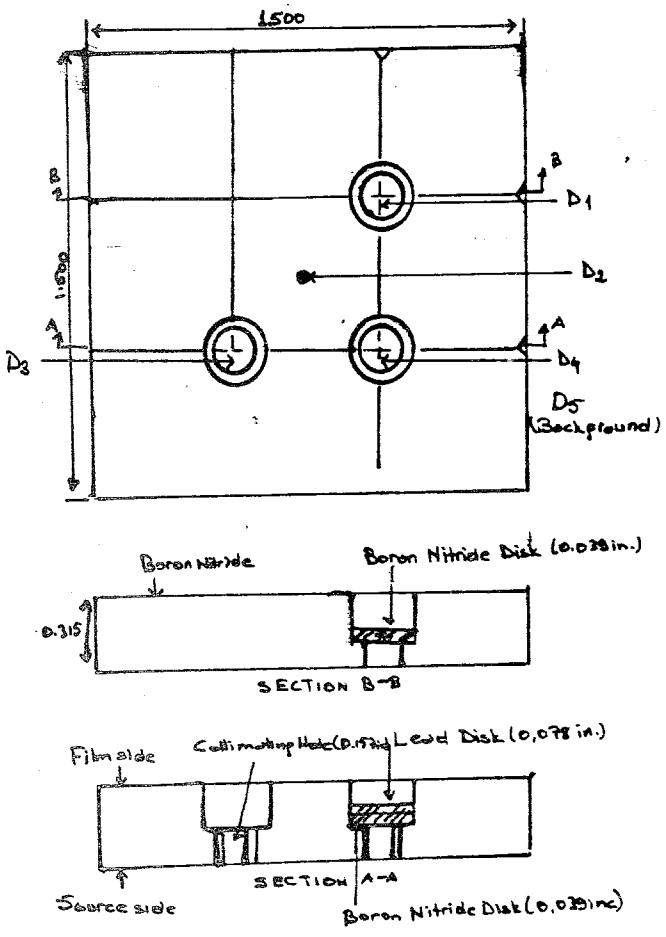

Figure 5.8. Beam purity indicator (25).

This image quality indicator is placed on a side of radiographing object and exposed to produce a background film density at the side of IOI from 2 to 3 density unit. Then with a densitometry density measurements are taken on the radiograph of the IOI at five positions from D_1 to D_5. These five measurements on the density of its image are recorded to give the information indicated in the Table (5.2).

TABLE 5.2. Information from ASTM Beam Purity Indicator (3).

Thermal neutron content (%)	$(D_3-D_1)/D_3 \times 100$
Scattered neutron content (%)	$(D_5-D_1)/D_3 \times 100$
Epithermal neutron content (%)	$(D_1-D_2)/D_3 \times 100$
Low energy gamma content (%)	$(D_1-D_4)/D_3 \times 100$

The presence of boron nitride in the beam purity indicator makes measurements regarding total neutron exposure, neutron energies and scattering factor involved in that exposure possible and the presence of lead makes measurements regarding gamma exposure and its energy possible.

The second type of IOI is used as sensitivity indicator and based on the detection of holes through different thickness of plastic step wedge (see Fig. 5.9).

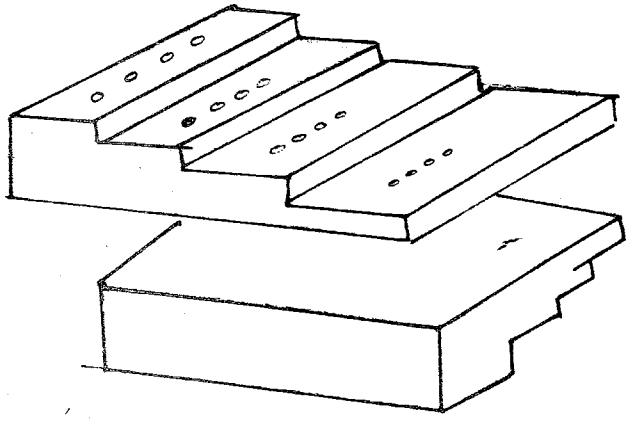

Figure 5.9. Sensitivity indicator (25).

The numerical designation of image quality is in the firm of, for example, N 75-10-6 indicating that a radiograph quality with a thermal neutron content of at least 75 percent, a scattered neutron of not more than 10 percent and a sensitivity such that a 0.02 inc dia x 0.02 in deep hole can be seen through 0.062 inc in plastic absorber (25).

5.4. Some Recommendations for Thermal Neutron Radiography

Generally a neutron radiography facility which is most suitable for carriying out the required detection or measurement operations should be used.

This depends on, at first, the type of neutron source. However, one must also consider the advantages of optimizing the geometry, beam quality, neturon energy and detection system whenever the radiography facility allows these parameters to be controlled.

Some advantages of geometry have been considered in the previous chapters. In general to obtain a high quality radiograph the collimator ratio (L/D) should be 100 or higher in case of reactor fuil inspecting, for a useful resolution this ratio should be 10 or greater. Collimator ratios of 50 or greater are recommended for most practical applications. (2).

The desirable characteristics of neutron beam for good radiographic applications would include: high thermal neutron intensity around 10^6 n/cm^2-sec or higher, relatively low fast neutron intensity with cadmium ratios of 24, or higher, low gamma-intensity with the ratio of thermal neutron intensity in n/cm^2-sec to the gamma radiation intensity in MR/sec of 10^5 n/cm^2-MR or higher in case of metal screen image detection, and 10^4 n/cm^2-MR or higher for scinllator image detection. Although its desirable to use a high cadmium ratio for thermal neutron radiography, there are some applications, inspection of reactor fuel elements, in which high epithermal or resonance neutron percentages would be invented.

For high resolution requirements metal converter screens should be used, and in case of high gamma intensity transfer exposure converter screens are usually preferred.

For high speed and low neutron intensity, scintillator converter screens are the better choice (5), (2).

CHAPTER VI

DESIGN OF NEUTRON RADIOGRAPHIC CAMERA

A neutron radiographic camera is designed to provide a large order thermal neutron flux at the image plane and consists of five basic components: neutron source, moderator, shield, collimator and imaging system.

A neutron radiographic camera system containing 3-curi ^{241}Am-Be isotopic will be decsribed in this chapter.

6.1. Source

The source is 3 Ci ^{241}Am-Be and is produced by double encapsulation in 304 stainless stell by J.L Shephord and Associates. This source has been tested and classified by ANSI procedures by producer.

The characteristics of the source are as follows: The neutron yield is 6.6×10^{6} n/sec isotropically. The exposure rate of 0.06 Mev gamma radiation from encapsulated source at one meter from the source is 6.6 mr/hr. The exposure of 4.4 Mev -γ- from Am(α,n)Be reaction for the same condition is 0.264 mr/hr. The sizes of source are 1" odx1.12" lenght. This source is fastened to the bottom of a methacrylate bar as shown in the Figure 6.1.

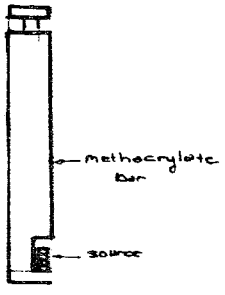

Fig. 6.1. Neutron source and its handle.

Figure 6.2. shows the energy spectrum of (Am-Bc) neutrons. Their average energy is about five MeV.

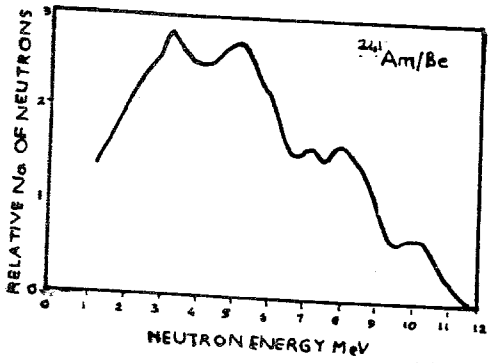

Fig. 6.2. Neutron energy spectra of ^{241}Am-Be Source (26).

6.2. Moderator

As has already be an indicated that the source must be surrounded with a material to slow down the fast neutrons to thermal energies. Since radioisotope neutron sources have relatively small neutron output, moderator material and dimensions must be such as to provide the highest possible peak thermal neutron flux over relatively small region of the collimator input. This fact is measured by thermalization factor which is defined by the ratio of the fast neutron yield to peak thermal flux. Some of thermalization factors for different source and materials are given in Table 6.1. The values in the table were collected from different experimental procedures and therotical analysis from several sources as indicated. (27), (3).

TABLE 6.1. Thermalization Factors for Different Moderators and Sources.

PLACE	SOURCE	H_2O	BeO	CH_2	Metal Hydride
ANL (calculated)	Am^{241}-^{242}Cm-Be	600	400	-	-
ANL (measured)	Am^{241}-Cm-Be	200	280	-	-
Univ. of Birm. (calculated)	Am^{241}-Cm-Be	200	280	-	-
ANL (calculated)	Cf^{252}	70	200	-	-
ORNL (calculated)	Cf^{252}	75	1400	-	-
WAD CO (calculated)	Cf^{252}	885	-	855	516

Among the moderator materials metal hydrides are the best moderators because of their high hydrogen content per cubic centimeter as compared to an equal valume of water and paraffin and their ability to be heated to $1273^{o}K$ and cooled to less than $10^{o}K$. However, economical considerations prove paraffin and water to be the most useful moderators. Therefore we used paraffin as moderator

To find the place of peak thermal neutron flux and the highest possible thermalization factor, a theoretical analysis was done in three different ways. The parameters used to calculate thermal neutron distribution in paraffin are given in the table.

TABLE 6.2. Diffusion Parameters for Thermal Neutrons (28).

Density (gr/cm^3)	D (cm)	Σa cm^{-1}	L (cm)	d_{tr} (cm)	extrapolated distance	Removal Cross section for 5 Mev
0.89	0.106	0.026	2.14 cm	0.32	0.227	0.161

6.2.1. Removal Diffusion Combination

In hydrogeneus medium, it was observed that the plot of the thermal flux from a fast neutron source closley paralels the fast neutron dose curve. This paralelism indicates that the thermal neutrons at any given point must have arisen from the slowing down of fast neutrons in the immediate vicinity of the observation point. One can therefore consider. The fast flux in a very small region as being the source of thermal neutrons. The reason is, a fast neutron emitted with energy of E_o in an ifinite hydrogeneus medium undergoes its first collision after moving one mean free path, ie. the distance $1/\Sigma_s(E)$. At this point neutron loses much of its energy therefore the cross section for second collision is now much larger, and the second mean free path is considerably shorter than the first. Hence the mean free path decreases with each encounter with the result that the neutron migrates only a short distance from the point where it was first scattered.

It will be seen in the shielding section that fast neutron flux at any point can be determined by removal theory. According to this model the removed neutrons are considered as a source for thermal neutrons (29).

The system of equations are

$$\phi_f(r) = -\frac{S\, e^{-\Sigma_r r}}{4\pi r^2} \qquad (6.1)$$

$$D\frac{d^2\phi_{th}}{dr^2} + \frac{2}{r}\frac{d\phi_{th}}{dr} - \Sigma_a\phi_{th} = -\frac{\Sigma_r S e^{-\Sigma_r r}}{4\pi r^2} \qquad (6.2)$$

where

$\phi_f(r)$ is the fast flux at position r

$\phi_{th}(r)$ is the thermal flux at position r

S is the source of fast neutrons

Σ_r is the removal cross section

Σ_a is the absorbtion cross section for thermal neutrons

D is the diffusion coefficient of thermal neutrons

Eq (6.2.) is the second order linear non-homogeneous diff-equation. In order to solve (Eq. 6.2.), it is convenient to introduce a new variable u, for homogeneous part of Eq. (6.2), defined by

$$u = r\phi$$

$$\frac{d^2u}{dr^2} - K^2u = 0 \qquad (6.3)$$

where

K is $\sqrt{\frac{\Sigma a}{D}}$

The solutions of Eq. (6.3.) are

$$\phi_{h1}(r) = A\frac{e^{-Kr}}{r}$$

$$\phi_{h2}(r) = B\frac{\text{Sinh } Kr}{r}$$

The Wronskian of these functions can be found to be $\frac{K}{r^2}$, and the general solution to the dif-equation is.

$$\phi th(r) = A\frac{e^{-Kr}}{r} + B\frac{\text{Sinh}Kr}{r} + \frac{\Sigma_r S}{4\pi DK}\left(\frac{\text{Sinh}Kr}{r}\int_a^r \frac{e^{-(\Sigma_r-K)r'}}{r'}dr' + \frac{e^{-Kr'}}{r'}\int_b^r e^{-\Sigma_r r'}\frac{\text{Sinh}Kr'}{r'}dr'\right) \quad (6.4)$$

To find the thermal flux through out the medium, boundary conditions of the medium must be imposed on Eq. (6.4.)

Let us first consider the medium to be of infinite extent, in this case the boundary conditions are;

1) $\phi_{th}(r)$ must remain finite at r=o

2) $\phi_{th}(r)$ must vanishe as $r\to\infty$

Therefore the limits a an b on the integrals and the constant in Eq. (6.4.) must be chosen in such a manner that the boundary conditions above are satisfied[x]

From equation four one can see that A=0, B=0, a=∞ and b=o

Then

$$\phi_{th}(r) = \frac{\Sigma_r S}{4\pi DK}\left(\frac{\text{sinh}Kr}{r}\int_r^\infty \frac{e^{-(\Sigma_r+K)r'}}{r'}dr' - \frac{e^{-Kr'}}{r'}\int_o^r e^{-\Sigma_r r'}\frac{\text{sinh}Kr'}{r'}dr'\right)$$

Applying some simple algebra, gives

$$\phi_{th}(r) = \frac{\Sigma_r S}{4\pi DK}\left(\frac{\text{Sinh}Kr}{r}\int_r^\infty \frac{e^{-(\Sigma_r+K)r'}}{r'}dr' - \frac{e^{-Kr}}{2r}\left(\int_o^\infty \frac{e^{-(\Sigma_r+K)r'}}{r'}dr' - \int_o^r \frac{e^{-(\Sigma_r-K)r'}}{r'}dr'\right.\right.$$

$$\phi_{th}(r) = \frac{\Sigma_r S}{4\pi DK}\left(\frac{\text{Sinh}Kr}{r}\int_r^\infty \frac{e^{-(\Sigma_r+K)r'}}{r'}dr' - \frac{e^{-Kr}}{2r}\left(\int_o^\infty \frac{e^{-(\Sigma_r+K)r'}}{r'}dr' - \int_r^\infty \frac{e^{-(\Sigma_r-K)r'}}{r'}dr'\right)\right.$$

$$\left. - \int_o^\infty \frac{e^{-(\Sigma_r+K)r'}}{r'}dr' + \int_r^\infty \frac{e^{-(\Sigma_r+K)r'}}{r'}dr'\right)\Big) \quad (6.5)$$

---

[x]Although there appears to be four unknown constants, there are only two because a and b can not be chosen independantly of A and B and vice versa.

To evaluate the integrals in Eq. (6.5), two new variables, p and q defined by $p = (\Sigma_r + K)r$ and $q = (\Sigma_r - K)r$, is introduced so that

$$\phi th(r) = \frac{\Sigma_r S}{4\pi DK}\left(\left(\frac{\sinh Kr}{r}\int_{(\Sigma_r+K)r}^{\infty}\frac{e^{-p}}{p}\,dp\right) - \frac{e^{-Kr}}{2r}\left(\int_0^{\infty}\frac{e^{-q}}{q}\,dq - \int_{(\Sigma_r-K)r}^{\infty}\frac{e^{-q}}{q}\,dq\right.\right.$$

$$\left.\left.\int_0^{\infty}\frac{e^{-p}}{p}\,dp + \int_{(\Sigma_r+K)r}^{\infty}\frac{e^{-p}}{p}\,dp\right)\right) \qquad (6.6)$$

These integrals are in the form of what is known as the exponantial integral function defined by

$$En(x) = x^{n-1}\int_x^{\infty}\frac{e^{-u}}{u^n}\,du$$

Inserting for the SinhKr term in Eq. (6.6)

$$\phi th(r) = \frac{\Sigma_r S}{8\pi DK}\left(\frac{e^{Kr}}{r}E_1((\Sigma_r+K)r) - \frac{e^{-Kr}}{r}E_1((\Sigma_r-K)r)\right) \qquad (6.7)$$

A plot of $\phi th(r)$ as function of r is given in Fig. 6.5.

Since the actual case is of a finite medium, the same problem was considered also for talking case.

This time the boundary conditions become such that ϕ_{th} must be finite at a r=o and be zero a=R, where R is the extrapolated boundary.

Writing the general solution once more

$$\phi th(r) = A\frac{e^{-Kr}}{r} + B\frac{\sinh Kr}{r} + \left(\frac{\Sigma_r S}{4\pi DK}\left(\frac{\sinh Kr}{r}\int_a^r\frac{e^{-(\Sigma_r-K)r'}}{r'}dr' + \frac{e^{-Kr}}{r}\int_b^r e^{-\Sigma_r r'}\frac{\sinh Kr'}{r'}dr'\right)\right)$$

(6.4)

To satisfy the above boundary conditions one can see that A=0 and b=0,

Then equation (6.4) becomes

$$\phi_{th}(r) = B\frac{\sinh Kr}{r} + \frac{\Sigma_r S}{4\pi DK}\left(\frac{\sinh Kr}{r}\int_r^R\frac{e^{-(\Sigma_r-K)r'}}{r'} - \frac{e^{-Kr}}{r}\int_0^r\frac{e^{-\Sigma_r r'}}{r'}\sinh Kr'\,dr'\right) \qquad (6.8)$$

Where B can be found from

$$-B\,\mathrm{Sinh}KR + \frac{\Sigma_r S}{4\pi DK} e^{-KR} \int_0^R \frac{e^{-\Sigma_r r'}}{r'} \mathrm{Sinh}Kr' dr' = 0 \qquad (6.9)$$

The integrals inequation (6.8) and (6.9) can be evaluated by converting these equations into the form of exponantial integral function.

Rearrangin equation (6.8), the thermal flux becomes

$$\phi_T(r) = B\frac{\mathrm{Sinh}Kr}{r} - \frac{\Sigma S}{8\pi DK}\frac{1}{r}\left\{ e^{Kr}\left(E_1((\Sigma_r+K)r) - E_1((\Sigma_r+K)R)\right) + e^{-Kr}\left(E_1((\Sigma_r+K)R) - E_1((\Sigma_r-K)r)\right)\right\} \qquad (6.10)$$

A plot of this, function for various moderator radius is given in Fig. (6.6) and the diffusion contstans used in equation (6.7) and (6.10) are given in Table (6.2).

It has been found that after 15 cm the thermal flux behaves almost as it does in the infinite medium. Therefore it is not practical to take the moderator dimensions greater than this value.

6.2.2 Two Group Diffusion Theory

In this method, also, neutrons are splitted into two groups. Thermal neutrons are included in one group called the thermal group and all the other neutrons are included in the fast group, such that.

$$\phi_2\ 1) = \int_0^{\sim 5kT} \phi(r,E)\ d\ E \text{ and}$$

$$\phi_2(r) = \int_{\sim 5kT}^{\infty} \phi(r,E)\ d\ E$$

---

a: is chosen as R arbitrarylv

The diffusion equations describing the fast and thermal neutron behavior are

$$D_1 \nabla^2 \phi_1 - \Sigma_1 \phi_1 = 0 \tag{6.11}$$

$$D_2 \nabla \phi_2 - \Sigma a \phi_2 + \Sigma_1 \phi_1 = 0 \tag{6.12}$$

where

Σ_1 is overall absorbtion cross section for fast group
Σ_2 is the absorbtion croos section for thermal group
D is the diffusion constant for fast group
D is the diffusion constant for thermal group

The fast diffusion coefficient D_1 is defined by

$$D_1 = \frac{\int_{\sim 5kT}^{nkT} D(E)\, dE/E}{\int_{\sim 5kT}^{nkT} \frac{dE}{E}}$$

In the absence of resonance capture, neutrons are not absorbed in the fast group, but they disappear from the fast group as a result of elastic and inelastic scatterings. Therefore by analogy to $L^2 = D/\Sigma a$, the quantity D_1/Σ_1 must be equal to one sixth the average of the square of the crow flight distance from the source to the point where a neutron leaves the fast group, that is, to the point where the neutrons slow down into the thermal group.
This however is precisely the definition of the neutron age so.

$$\frac{D}{\Sigma_1} = \Gamma_t$$

where Γ_T is the fast neutron age to thermalization (30).
The solutions of these dif-equations are

$$\phi_1 = A_1 \frac{e^{-r/\sqrt{\Gamma_t}}}{r} - A_2 \frac{e^{-r/\sqrt{\Gamma_t}}}{r}$$

$$\phi_2 = B_1 \frac{e^{-r/L}}{r} + B_2 \frac{e^{-r/L}}{r} + \frac{LS}{D_2 8\pi\tau_t} \left\{ \frac{-e^{r/\sqrt{\tau}} 2L\tau_t}{r \quad (L^2-\tau_t)} - \frac{e^{r/L} \; L\sqrt{\tau_t}}{r \quad (\sqrt{\tau_t}-L)} \right\}$$

The boundary conditions are

$$\lim_{r\to o} 4\pi r^2 J_1 = S \text{ and } \lim_{r\to\infty} \phi_1(r) = 0$$

$$\lim_{r\to o} 4\pi r^2 J_2 = 0 \text{ and } \lim_{r\to\infty} \phi_2(r) = 0$$

It will be seen from the boundary conditions that the geometry is of a point source in an infinite medium.

Applying the above boundary conditions one can find that:

$$A_1 = \frac{S}{4\pi\tau_t \Sigma_1}, \quad B_2 = 0 \text{ and } B_1 = -\frac{LS}{D_2 8\pi\tau_t} \left(\frac{2\tau_t}{L^2 \tau_t} - \frac{L\sqrt{\tau_t}}{\sqrt{\tau_t}-L} \right)$$

Hence the fast and thermal fluxes are:

$$\phi_1(r) = \frac{S}{4\pi r \tau_t \Sigma_1} \exp\left(-r/\sqrt{\tau}\right) \tag{6.13}$$

$$\phi_2(r) = \frac{SL^2}{4\pi r D_2 (L^2-\tau_t)} \left(\exp(-r/L) - \exp(-r/\sqrt{\tau_t}) \right) \tag{6.14}$$

A plot of $\phi_2(r)$ as a function of r is given in Figure 6.6

6.2.3. Removal Age Combination

In the removal- diffusion combination the removed neutrons are considered directly as source for thermal neutrons which then diffuse in the medium.

However in the removal-age combination, the removed neutrons are not considered to be direct source of thermal neutrons; the slowing clown of neutrons after removal collision is taken into consideration according to the fermi age model. The diffusion of thermal neutrons is neglected and the slowing down density is set equal to the absorbtion rate.

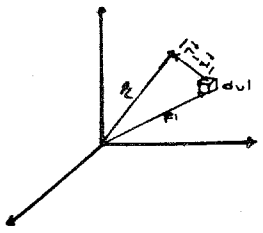

Fig. 6.3. Geometry for computing the flux from distributed source in an infinite medium.

According to the removal theory, each time the fast neutrons undergo a removal collison it is assumed to contribute to an isotropic slowing down source. If $G(r^1)$ is the fast flux from a point at distance r^1 from selected referance frame shown in Fig. (6.3) the volume source $P(r^1)$ of slowing down density is $-\frac{dG(r^1)}{dr^1}$, which is equal to

$$P(r^1) = \Sigma_r \frac{e^{-\Sigma_r r^1}}{4\pi r^2}$$

Further more according to the Fermi age model the slowing down-density $g(r, r^1, \tau_t)$ at a point r from a unit source located at r^1 is

$$g(r, r^1, \tau_t) = \frac{e^{-|\vec{r}-\vec{r}^1|^2/4\tau_t}}{(4\pi\tau_t)^{3/2}} \qquad (6.15)$$

Then the total slowing down density to thermal range is

$$\theta(r,\tau_t) = \int P(r^1)\, g\,(r, r^1, \tau_t)\, dv^1 \qquad (6.16)$$

Neglecting the diffusion of thermal neutrons, the thermal neutron absorbtion rate becomes

$$\Sigma a\phi_{th} = \theta\,(r,\tau_t)$$

$$\theta(r,\tau t) = \frac{\Sigma_r S}{2(4\pi\tau_t)^{3/2}} \int_0^{\infty}\int_e^{\infty} e^{-\Sigma_r \tau} \, e^{-\left(\frac{r^2 - r^{1 2} - 2rr^1 \cos\theta}{4\tau}\right)} \sin\theta d\theta \, dr^1 \qquad (6.17)$$

By making the transformotion $\mu = \text{Cos}\theta$ and $d\mu = -\text{Sin}\theta d\theta$, and integrating with respects $d\mu$, one obtain.

$$\theta(r,\Gamma t) = \frac{\Sigma_r S}{(4\pi\Gamma)^{3/2}} \frac{1}{r}\left(\int_0^{\infty} \frac{e^{\frac{-4\Gamma\Sigma_r r'-r^2-r'^2-2rr'}{4\Gamma t}}}{r'} dr' - \int_0^{\infty} \frac{e^{\frac{-4\Gamma\Sigma_r r'-r^2-r'^2-2rr'}{4\Gamma t}}}{r'} dr'\right) \tag{6.18}$$

Although limits on the integral must be carried from zero to infinete, as an approximation, limits have been adjusted for hallow source finite medium as shown in the figure

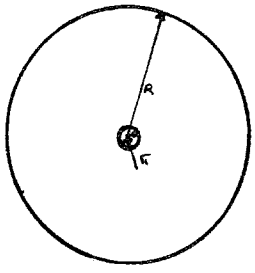

Fig. 6.4. Geometry for computing thermal flux according to Removal-Age theory

The final form of $\theta(r,\Gamma_t)$ is

$$\theta(r,\Gamma_t) = \frac{\Sigma_s S}{(4\pi\Gamma)^{3/2}} \frac{e^{\Sigma r_1}}{r} \int_{r_1}^{R} \frac{e^{\frac{-4\Gamma\Sigma_r r'-r^2-r'^2-2rr'}{4\Gamma t}}}{r'} dr' - \int_{r_1}^{R} \frac{e^{\frac{-4\Gamma\Sigma_r r'-r^2-r'^2-2rr'}{4\Gamma t}}}{r'} dr' \tag{6.19}$$

Setting the slowing down density to thermal absorbtion rate

$$\Sigma a \phi_{th}(r) = \theta(r,\Gamma_t)$$

The thermal flux will be

$$\phi_{th}(r) = \frac{\theta(r,\Gamma t)}{\Sigma_a} \tag{6.20}$$

The integral in equation 6.19 has been computed numerically by means of Shimpshon rule and the thermal flux distribution so obtained is given in the Figure 6.6.

To compare the calculated thermal flux with experimantely determined flux values Figure 6.7 has been presented.

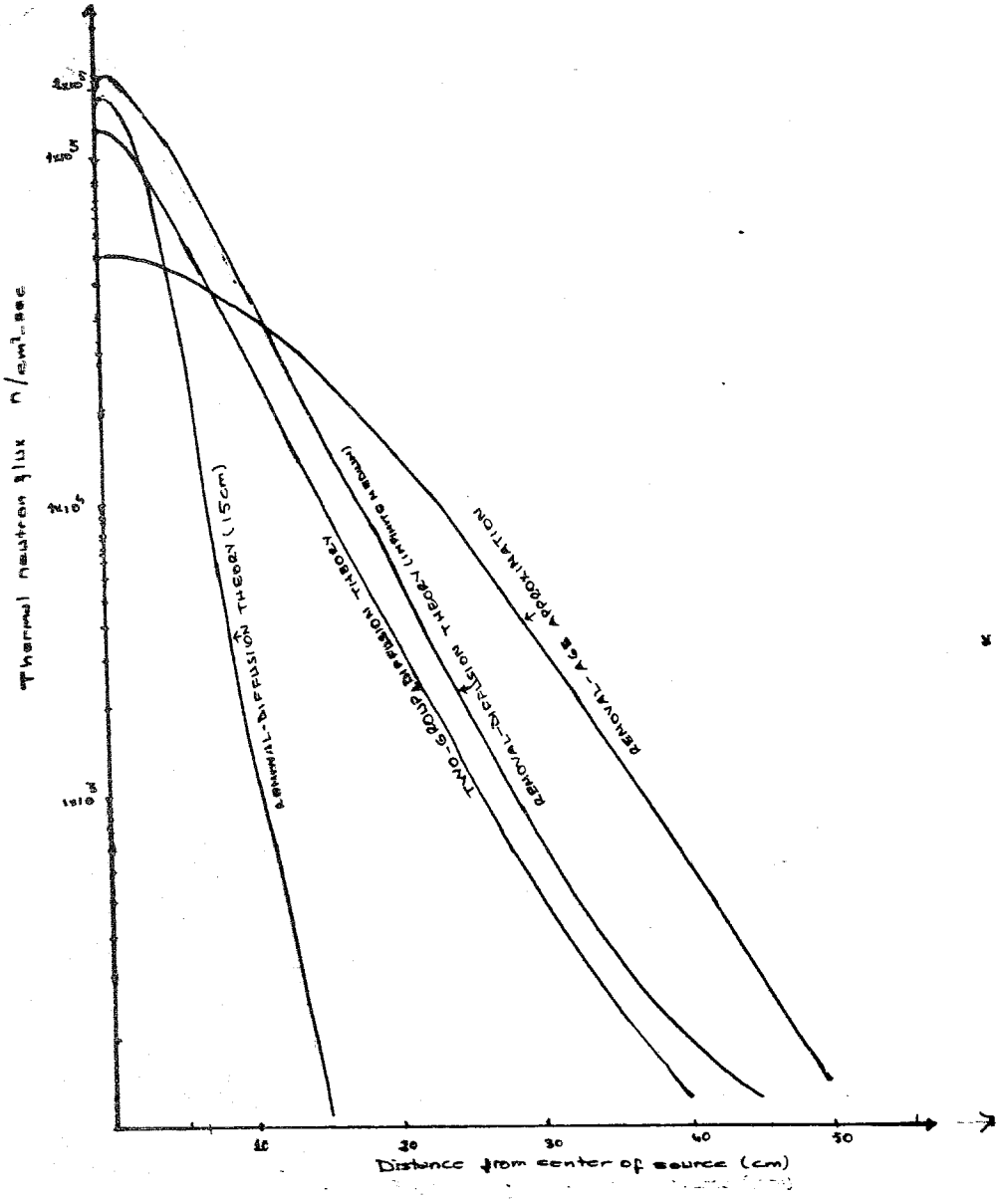

Fig. 6.5 Thermal neutron flux distribution calculated from three models.

Thermalization factors obtained from three approximation are given in table

TABLE 6.3 Thermalization Factors Obtained from Three Method

METHOD	THERMALİZATION FACTOR
Removal-Diffusion	30
Two Group Diffusion	73
Removal Age	188

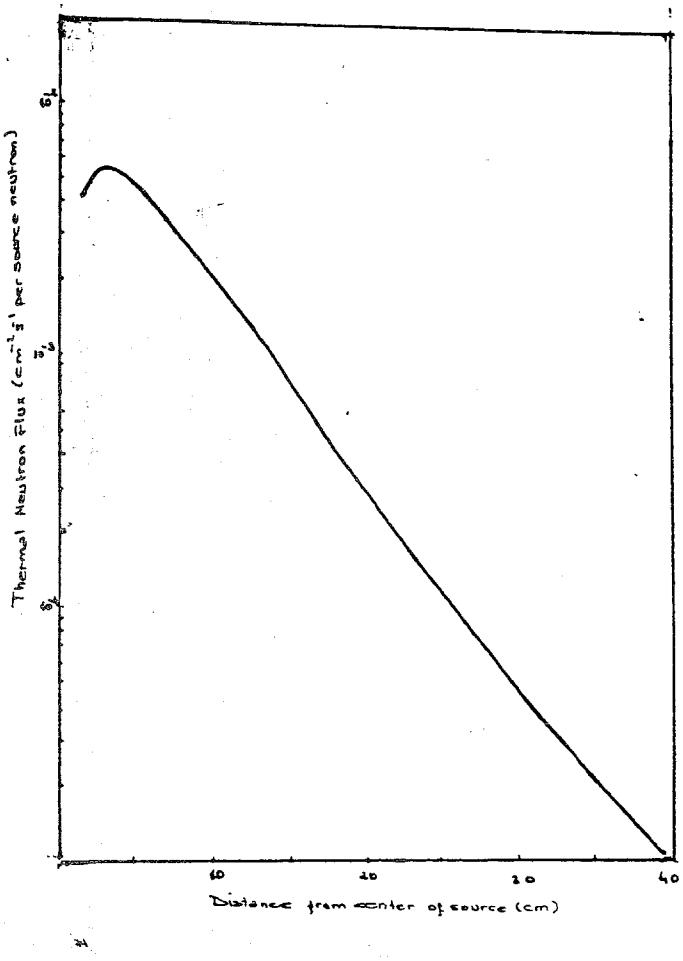

Fig. 6.7. Thermal neutron flux distribution (experimentally) produced by 1CiAm-Be source in a water moderator (3).

Although Fig. 6.7 shows the thermal neutron flux in water moderator the diffusion parameters of water follow closely those of parraffin.

6.3. SHIELD

The dimensions and therefore portability of a radiographic camera depends to a large extent on the biological shield. The most significant types of radiation for which shielding is required are neutrons and gamma rays.

Therefore it is necessary to design a shield involving a suitable shielding material and thickness to decrease the total radiation effectiveness to a permissible level.

Since meutrons are usually born at high energy level it is necessary to use a material which slows down neutrons and then captures them. During this capture process secondary radiation (capture gamma rays) are produced. This radiation is distributed through out the shield and is often the dominant contributer to the dose rate. Dense materials such as lead and iron to attenuate gamma rays and lights materials such as various hydrogeneous compounds to slow-down neutrons are normally used in combination. Concerate has been widely used as an in expensive shield, because it is a mixture of heavy and light elements but it is too bulky for a camera shield. The addition of boron or lithium to a hydrogeneus material such as polly-ethylene, parafin, water and water extended polyster, reduces both thermal neutron and capture gamma dose rates through the absorption reactions $^{10}B(n,\alpha)^{7}$ Li or $^{b}L_i(n,\alpha)T$ as well as attenuation of fast neutrons. Both reactions have higher cross section (3840 and 945 barns respectively) than the $H(n,\gamma)D$ reaction in the hydrogeneous material and result in less secondary gamma radiation. The 0.48 Mev gamma from the excited $^{7}L_i$ nuclide is also easier to attenuate than the 2.3 MeV gamma from hydrogen reaction, while no gamma rays at all are produced in the lithium reaction (31).

Since our neutron source intensity and energies of gamma rays are low, it was thoughtmore appropriate to enlarge the moderator dimensions than ussing such a mixture or concrete for shield. To attenuate gamma rays a steel cup surrounding the moderater was used.

6.3.1. Attenuation of Neutrons

Before considering shielding calculations, it is necessary to briefly look at the attenuation process of neutrons and gammarays. At firstneutron attenuation and dose rate calculations will be considered.

The attenuation of neutrons takes place by elastic and inelastic scattering as well as neutron capture reactions. Since probability of neutron capture is large at thermal energies, a considerable degredation in fast neutron energy must just take place before neutrons are removed by capture.

A considerable energy degredation takes place via elastic and inelastic scattering. In the inelastic scattering process the target necleus is raised to a quantum state above ground level (either through neutron assimilation and re emission or direct exitation), and the nucleus decays to the ground state by the emission of one or more gamma rays. The inelastic scattering process is only significant at energies greater than 0.5 MeV and for heavy nucleus. Therefore the presence of heavy elements in the shield is most effective in reducing the neutron energy by inelastic collision In the elastic scattering process, the nucleus is unchanged in either isotopic composition or internal energy after interacting with a neutron. In this process kinetic energy is conserved. Elastic scattering is largely significant at low energies and is more likely with decreasing energy, therefore, thermalization of neutrons takes place mostly via elastic scattering. Since the average energy loss per collision is large in each elastic collision with hydrogen and since the elastic scattering cross section at energies above 0.1 Mev increases rapidly with decreasing neutron energy, once a neutron in the source energy range under goes its first elastic collision, it rapidly undergoes additional elastic collisions and is thermalized.

The absorption process is significant only at thermal energy range for almost all elements, however, at high energies absorption process is slightly significant for heavy elements. After the absorbtion process a nucleus usually emits a gamma ray known as the capture gamma (32).

6.3.2. Shield Calculation Methods

To perform sufficiently accurate shielding calculations detailed information on the spatial and energy distribution of neutrons in a medium must be known. Some theoratical techniques are available for this purpose. The most accurate theoratical calculations can be accomplished by Boltzman kinetic equations. However the compliated structure of this equation makes it impractical for use for in shielding calculations and approximation methods become necessary. One of them is to write the Boltzman equation in the age diffusion approximation then solve this with multigroup method.

In this method the neutron energy or lethargy range is broken down into a number of energy ranges and neutrons in each energy range are treated as sparate group with its own eqe diffusion equation.

A simpler approach is to write the three group diffusion equations which are

$$\nabla D_1 \nabla \phi_1 - \Sigma_1 \phi_1 = 0$$
$$\nabla D_2 \nabla \phi_2 - \Sigma_2 \phi_2 + \Sigma s_1 \phi_1 = 0$$
$$\nabla D_3 \nabla \phi_3 - \Sigma_3 \phi_3 + \Sigma s_2 \phi_2 = 0$$

Three equations describe the fast, intermediate and the thermal fluxes respectively. The constants in these equations are determined experimantally.

However suitable they may be for usual reactor calculations, conventional age-diffusion theories have some drawbacks when applied shielding calculations. because neutrons under consideration are mostly, fast neutrons. Basically they require that the neutron angular flux be nearly isotropic, which is in general true for the low-energy scattered neutron but not for high energy neutrons. Also the solution holds only for distances not too far from the source.

However the neutrons of interest in the shielding work are of an energy muchgreater then the average, that much of the attention is concentrated around fast neutron penetration. Therefore the simple form of diffusion equation is not valid for fast neutron behavior.

Especially in hydrogeneous medium if a fast neutron suffers a collision with hydrogen, its energy, is on the average reduced by one half, and as already indicatedbefore because of the rapid increase in the cross section of hydrogen with increasingenergy, the mean free path of its second collision is greatly shortened. As a consequence, the neutron has its next collisions near the site of its first. In this way energy of the neutrons eventually fall below fast energy region and rapidly attenuated and absorbed near the site of their first collisions. Thus it follows that a single collision with hydrogen effectively removes a neutron from among the fast neutrons. Therefore the attenuation of fast neutron can be described with a removal cross section which is effectively equal to absorption

in a simple exponential form.

When experimental became available about 1950, Albert and Welton constructed a model which introduces the concept of removal cross sections to describe the attenuation of fast neutrons in hydrogeneus media. Their formulation for the fast flux in water from a point fission source is

$$\phi(r) = \frac{\int f(E)\, e^{-\Sigma_r^H r}\, e^{-\Sigma^O r(E)}}{4\pi r^2} \, dE$$

where $\phi(r)$ is neutron flux at a distance r
$f(E)$ is fission neutron spectrum
$\Sigma^H(E)$ is hydrogen cross section
Σ_r^O is energy indipendent removal cross section for oxygen

The assumption was that the entire cross section for hydrogen was effective for removel but only a certain fraction for heavier elements such as oxygen.

Their most careful experimantel studies showed that the fast neutron dose rate from a poit source deviates from a simple shaight line behavior when multiplied with r^2 and plotted on asemilog scale. In this case decay becomes some what steeper with increasing distance from the soruce. This originates from the fact that neutron scattering by hydrogen is strougly anisotropic in the forward direction in the laboratory system, therefore the penetiating component is likely to be composed largely of neutrons which have had one or more collisions but have suffered only a small angular deflection. This component may be much larger than the pure uncollided flux. There after the average energy of neutrons will sink some what and this fact explains the stepper decrease.

About 1957 spinnery conceived a method to predict the penetration of these neutrons which are neither seriously deflected nor reduced significantly, in energy by use of a simple "uncollided" kernel

$$\phi(r) = \frac{S\, e^{-\Sigma_r r}}{4\pi r^2} \qquad (6.21)$$

where

$\phi(r)$ is the removal flux

Σ_r is the removal cross section

The value of Σr is lessthen the total cross section Σt since the flux defined by the kernel includes those neutrons which have made glancing collisions.

It can be expressed as:

$$\Sigma_r = \Sigma_t - f\Sigma_s$$

Where

Σs is the elastic scattering cross section

f is the fraction of elastic collision which can be considered glancing

It will be noticed that with this kernel, a fraction of elastic collisions is ignored, and the changes of direction and energy of such collisions are assumed to be small.

With the energy dependence the removel flux as a function of energy is given by

$$\phi_r(E) = \frac{f(E)e^{-\Sigma_r(E)r}}{4\pi r^2} \qquad (6.22)$$

The removal attenuation method discussed above takes into account the most energetic neutrons The complete design of a shield requires, in addition, a knowledge of the spatial distribution of fast neutrons, thermal and all intermediate energies since they determine the sources of inelastic and capture gamma rays.

Therefore Spinney and subsequent workers combined the calculations with diffusion equations such that the removel calculation was used to describe the penetration of the forward directed neutrons and the diffusion equation is used to describe the migration following such collisions.

For radioactive neutrons sources the fast neutron dose rate is calculated using equation 6.21. or some modified form of it. In this equation the removel cross section is determined experimentl~ which gives the integrated value of removel cross section over source energy. (8)

6.3.3. Neutron Dose Rate Calculations

As indicated before since the dose rate from neutrons are mainly due to the fast component, the contribution from low and thermal energy neutrons are neglected

The dose rate from fast neutrons was calculated using the point source kernel given in equation (5.21) such that the dose rate from a point source at the surface of a shield material is, assuming all of neutrons born at average energy of five Mev,

$$D(r) = \frac{S\, f\, \xi}{4\pi r^2} \qquad \text{(mrem/h)} \qquad (6.23)$$

where ξ is the conversion factor which relates fast neutron flux to dose rate

F is the neutron attanuation factor for the shield material and is equal to $e^{-\Sigma_r \Gamma}$

F was computed in two different ways: the first one is experimentally determined at the Mound Laboratory. It has been found that the attenuation factor in water for neutrons from (n,α) sources can be correleted as $f = e^{-.11t}$ The attenuation factor for shield containing more than 40 atom percent hydrogen can be obtained by a ratio of the hydrogen content of the shield to that in water times the exponent of the neutron attenuation factor for water (33). Since paraffin has more than 40 atom percent hydrogen so the neutron attenuation factor can be estimated by the hydrogen ratio method as follows

$$\frac{H_{paraf.}}{H_{w.}} = \frac{7.9 \times 10^{22}}{6.7 \times 10^{22}} = 1.179$$

Then applying the hydrogen ratio to the neutron attenuation factor for water, the neutron attenuation factor parafin will be

$$f = e^{-11.1.179t} = e^{-.129t}$$

In the second approach value of the removal cross section for fast neutrons from Am Be source was taken to be that of Po-Be source which is equal to 0.161 cm^{-1}. Blizard recommends the use of a value of 5 for the build up factor B for Po-Be sources with water or parafin shields more than 20 cm in thinkness (34).

$$f = e^{-.161.t}$$

Another way to compute dose rates is from Figure 6.7 which shows fast neutron attenuation in containers of paraffin and water

At first flux and dose rate is determined at a given distance from unshielded source according to equation (6.23), in which case f=1 Then with the aid of Fig. 6.7 the dose rate at any distance from shielded source is found by the product of attenuation factor and the unshielded dose Figure 6.8. shows neutron dose rate for various thickness of paraffin shield.

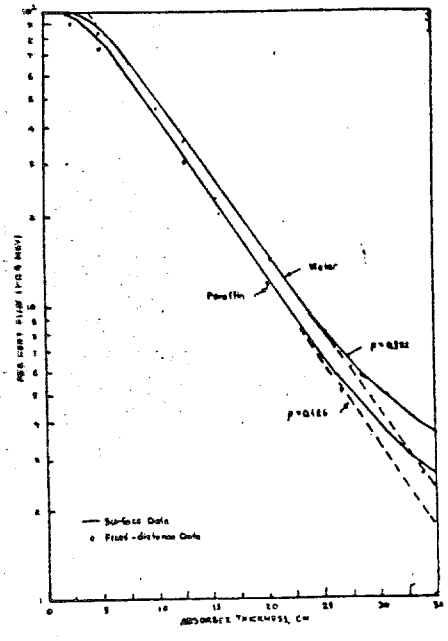

Fig. 6.7. Fast-neutron attenuation in cylindrical containers of paraffin and water (35)

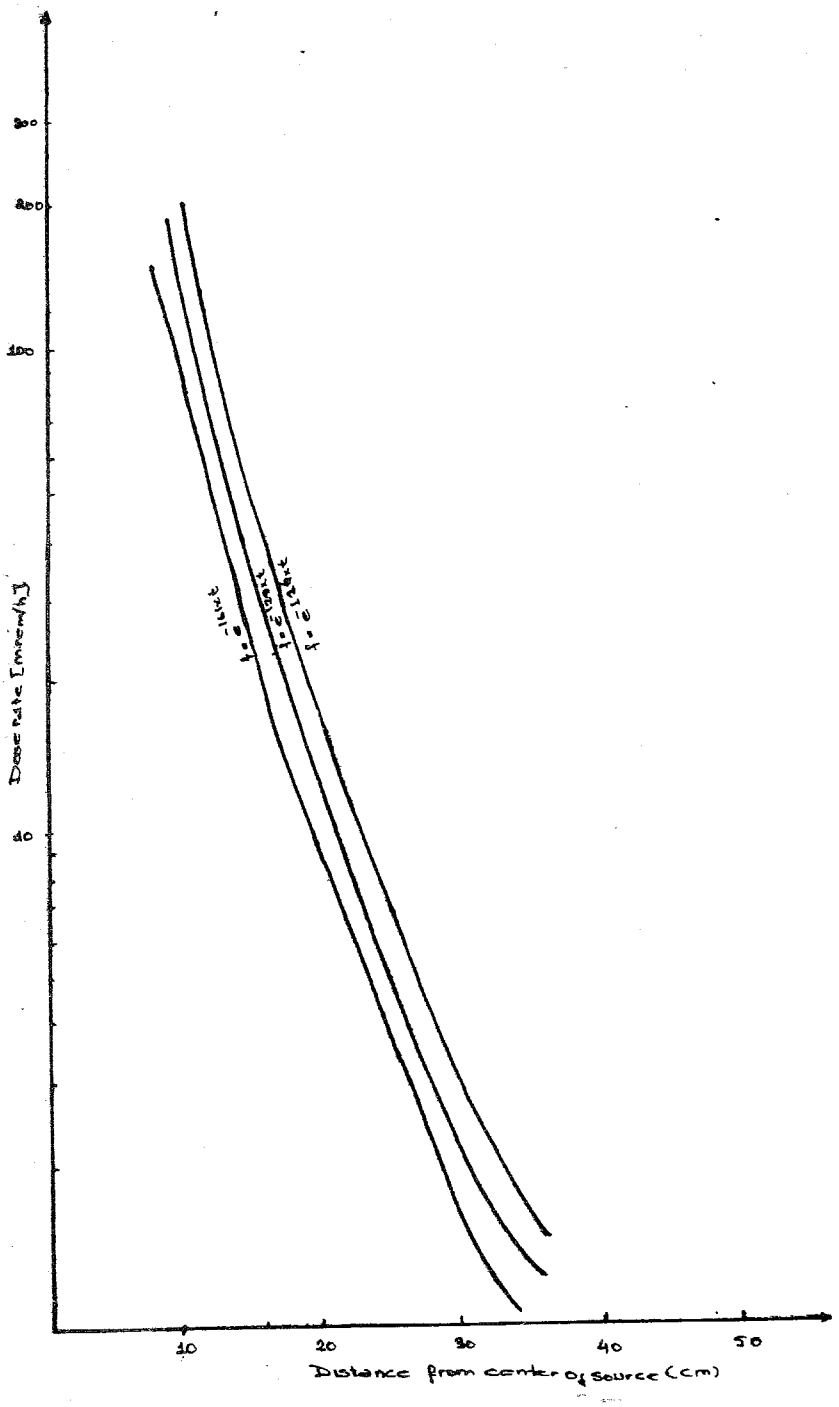

Fig. 6.8 Neutron dose rate calculated from three different ways.

6.3.4. Attenuation of Gamma Rays

The attenuation of gamma rays takes place mainly through three different interaction process. These are: a) photo electric effect, b) pair production, c) compton scattering

In the photo electric effect an incident photon transfers all of its energy to one of the atomic electrons, ejecting it from the atom. At low energies attenuation of photons is mainly due to the photoelectric effect which becomes more important as the atomic number Z of the absorber increases and as the photon energy goes-down.

In the pair production process all the energy of the incident photon is transfered into the creation of an electron pair-an electron and a positron. Since the rest mass of the pair is equal to 1.022 Mev the pair production process occurs only at photon energies greater than 1.022 Mev. pair production is effective at high energies and high atomic number.

In contrast with the preeceding interactions which are absorbtive processes, compton effect is a scattering process which alters the direction and energy of incident photons. Compton scattering is a predominant interaction over a wide energy region. Even for heavy elements it forms the major part of the attenuation coefficient from 0.5 to 5 MeV Especially in the very light elements the other two interaction are negligible except at exteremely low and high energies. Therefore such materials are said to be compton scatterers.

In spite of existence of many different types of interaction processes other than these cited above mainly these effect are considered in the shielding calculations and the total attenuation coefficient of gamma rays is taken as the sum of these three attenuation processes.

Since first of the two processes are absorbtive it is the compton effect which complicates the shielding calculations.

6.3.5. Calculation of Gamma Dose Rate

To calculate the gamma dose rate, following factors must first be determined. These are: a) the intensity and spectrum of gamma rays, b) total and energy absorbtion-mass attenuation cross sections for the shield material and the material in which the dose is to be determined, c) dose rate build up factor.

The intensity and spectrum of gamma rays: Gamma rays originate from the source itself through decay of Americium and its daughters, from (α,n) reaction and from obsorbtion of thermal neutrons by hydrogen and carbon through (n,γ) reaction. The total intensity of source gamma is 6.864 mr/hr at 1 m from unshielded source. On the average 6.6 mr/hr is due to the 0.06 MeV photon and the remaining part of 0.264 mr/hr is due to the 4.4 Mew photons. The gamma intensity arising from (n,γ) gamma reaction will be determined later. The energies of gammas from (n,γ) reaction for H and C are on the average 2.2 MeV and 4 MeV respectivelv.

Total and energy absorbtion mass attenuation coeff: The mass attenuation coefficient for shield materials prafin and Iron are given in the Table 6.4. Some of them was calculated by interpolation and some from formulation given below (8).

$$\frac{\mu}{g}(C_{25}H_{52}) - \frac{52M\ H}{52\ MH-25\ Mc}\ \frac{\mu}{g}(H) - \frac{52\ Mc}{52\ MH-25\ Mc}\ \frac{\mu}{g}(C)$$

where $\frac{\mu}{g}(C_{25}H_{52})$ is the mass attenuation coefficient for paraffin

$\frac{\mu}{g}(H)$ is the mass attenuation coefficient for hydrogen

$\frac{\mu}{g}(C)$ is the mass attenuation coefficient for carbon

M_H, Mc are atomic weight of hydrogen and carbon respectively

TABLE 6.4. Values of Mass Attenuation Coefficient μ/g cm^2/g for Shield Materials (8).

PHOTON ENERGY Mev	H	C	$C_{25}H_{52}$	Fe
0.06	0.326	0.170	193	1.13
2.2	0.0838	0.0427	0.0488	0.04122
4	0.581	0.0305	0.346	0.0331
4.4	0.055	0.0291	0.0329	0.0324

TABLE 6.5. Values of Energy Absorbtion-Mass Attenuation Coefficient, $\mu a/\rho$, cm^2 for Air (8).

PHOTON ENERGY	Air
0.06	0.0287
2.2	0.023226
4	0.0194
4.4	0.01888

Dose Build-up factor: It is necessary to introduce a build-up factor in the dose rate calculations to compansate for those photons which are only degraded energy rather than being removed. The build-up factor can be chosen from appropriate tables for source energy per photon, material and thikness of shield, attenuation coefficient for source energy and geometry of the shield.

The principle advantage of expressing attenuation properties of media in the form of $\phi = B\phi_0 e^{-\mu t}$ is that the build-up factor varies rather slowly with respect to changes in attenuation distance, source photon energy and average atomic composition. It is thus possible to interpolate rather accuratelyfor values B and to obtain solutions for attenuation problems from another limited number of actual calculations.

Build-up factors were used for dose rate calculations arising from source itself. The build-up factors for point source geometry and various thickness of shield material are given in the Table 6.6. Some of these build up factors were calculated by means of interpolation. Also for some energies at which exposure build up factor was not found, the energy deposition build up factor was used as the exposure build-up factor[x] and the build-up factor for parafin was taken to be the build-up factor for water.[xx]

---

[x] Type of the instrument response must be specified in order to establish the build up factor precisely. However, if the responses are closley related, such as energy fluence, exposure and absorbed dose (energy deposition), the corresponding build-up factors will always be of the same order of magnitude and will often be very close to one another (8).

[xx] In many instances the elements involved are so close in z that the shielding characteristic of the mixture properties are obvious for example in gamma ray build-up fa tor between CH_2 or CH and water is probably too small to be of significance in shielding problems (32).

TABLE 6.6. Exposure Build-up Factor for Point Isotropic Source, Infinite Medium for Water (8).

Eo	r-10	r-15	r-20	r-25	r-30	r-35	r-40	r-45	50
Mev	1.71	2.56	3.42	4.27	5.13	5.98	6.84	7.69	8.55
0.06	9.43	17.15	26.14	37.09	52.31	67.53	82.75	105.15	129.20
4.4	-	-	-	-	-	1.56	1.66	1.74	1.83

Since dose rate is an additive quantity, the dose rate arising from source itself and those arising from (n, γ) reactions will be treated sparately.

Dose rate from source: Since source is embedded in parafin, point source geometry can be used to determine the flux density and the dose rate through out the medium[x]

Gamma flux at any point in the medium is given by

$$\phi(r) = B \frac{Se^{-\mu r}}{4\pi r^2} \qquad (6.23)$$

where $\phi(r)$ is the gamma flux at point r

s is the source strenght γ/sec

μ is the linear attenuation coefficient of the medium

B is the build-up factor

The relationship between dose rate interms of reontgen, D and gamma flux density for monoenergetic radiation of energy E is determined by the following formula

$$D(r) = \frac{\phi(r) E \mu_a 1.6\times10^{-6}}{88} \text{ (r/sec)} \qquad (6.24)$$

where

μa is the mass energy-absorbtion coefficient of gamma radiation in air cm^2/g

1.6×10^{-6} is the energy equivalent in ergs of 1 Mev

88 is the energy equivalent in ergs/gr of 1 reontgen

To find gamma flux, $\phi(r)$, gamma source strength must be known at any point.

Using equation (2) the gamma flux having the energy of 0.06 Mev, and 4.4 at 1 m from the source can be found from.

$$\phi = \frac{88.D}{E.\mu\ 1.6x10^{-6}} \qquad (6.25)$$

Placing the value of D, E, μ, one can find the value of the gamma flux at the desired distance. The gamma strength can be found from Eq. (6.24) assuming a particle flux build-up of unity.
To find the dose rate at the camera surface the following relation was used.

$$D(r) = Br \frac{S\ e^{-\mu_1 r}\ E\ a\ 1.6x10^{-6}}{4\pi r^2.88} e^{-\mu_2 d}\ 3600\ (r/hr) \qquad (6.26)$$

Where

μ_1 is the attenuation coefficient for parafin
μ_2 is the attenuation coefficient for parafin
d is the steel thickness which isconstant
Br is the exposure-build-up factor for parafin[x]
r is radius of the parafin block

Figure (6.9) shows the dose rate at the surface of the camera arising from 0.06 Mev and 4.4 Mev gamma radiations for fixed steel thickness, 0.5 cm.

Dose rate from (n,γ) reaction: The gamma dose rate from (n,γ) reaction comes from capture of thermal neutrons by hydrogen and carbon in paraffin. Determination of the dose rate of the capture gamma rays involves the source distribution. This distribution depends on thermal neutron distribution through out the medium.

---

[x] The exposure build-up factor sted has not been considered because of its small thickness

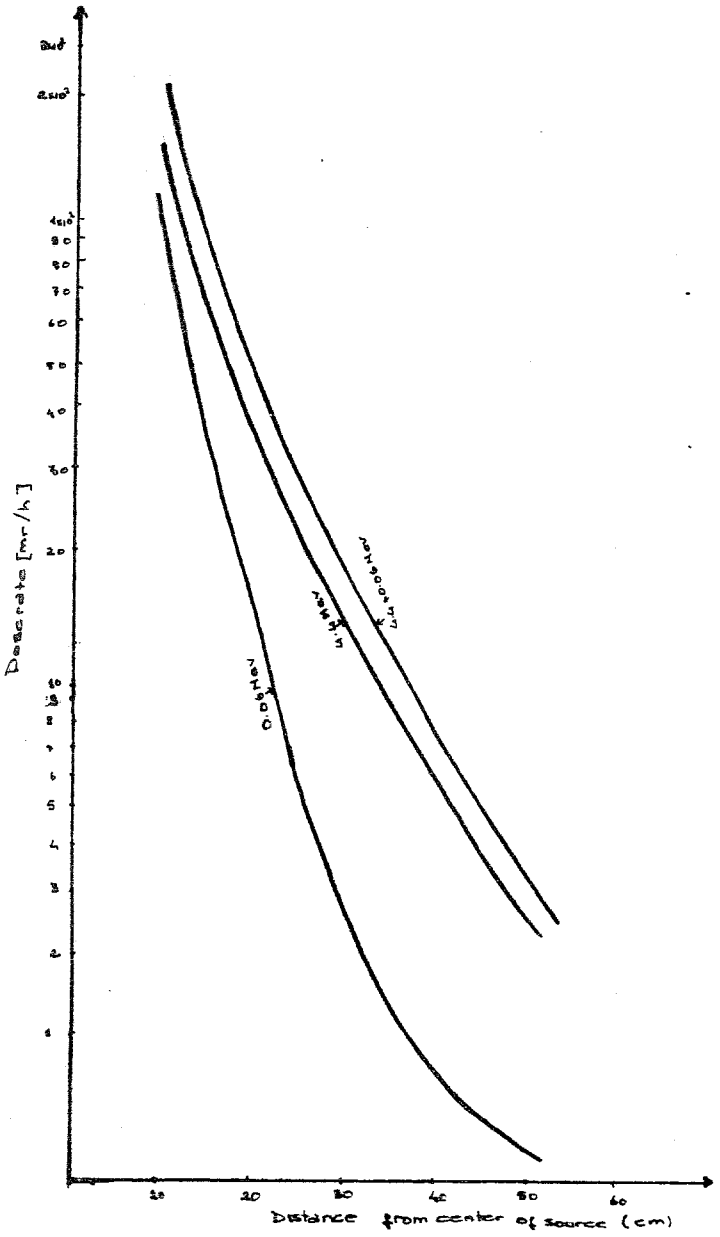

Fig. 6.9 The doserate at the surface of camera for varius thicnesses.

The thermal neutron flux distribution in the medium has been determined in the medium in three differentways. Two of them, removal diffusion, and two group diffusion equations, have been used to calculate the distribution of capture gammas. Then the distribution of capture gamma-ray photons of a specific energy can be found as

$$\phi_\gamma = \int_{V'} \frac{S_V(\vec{r}')}{\pi} G(p, s, \Sigma)^{x} \, dv'$$

---

x The function $G(p, s \Sigma)$ is given in reference (8).

where $S_v = \Sigma a \phi_{th}(r^1)$

Rather than solving this equation, an approximate approach, can more easily be employed. This is to use an average value for the gamma source strength and assume it to be constant through out the medium. Then using equation (6.27). Which gives the strength, S_a of an isotropic surface source which is equivalent to volume source of sternght S_v, the gamma particle for square centimeter per sec at the paraffin surface is obtained by (36)

$$Sa = \frac{Sv}{\mu} \qquad (6.27)$$

where S_v is the volume source strength, particle/cm^2 sec

μ is the total linear attenuation coefficient, cm^{-1}

This isotropic surface source gives the same dose at the steel exterior, it placed at the interface between the volume source (parafin block) and the shield (steel).

This method tends to overestimate the source strength of the equivalent surface source, since it gives equal weight to all parts of the volume distributed source. In actuality, most of the radiation reaching the parafin surface arises from regions of the paraffin block where the source strength is generally less then in the interior. However the dose rate obtained with this method will be on the sage side.

The average volumetric source strength is given by

$$\overline{S}_v = \frac{N \int_v \Sigma a(1)\phi(r)dV}{\int_v dV}$$

Where N is the number of photons of the specified energy produced per neutron capture

Σa is the macroscopic capture cross section of the medium

Assuming a constant and inserting the thermal flux distribution

obtained from two group diffusion theory[x], the average volumetric gamma source strength will be

$$\overline{S}_{v_1} = \frac{\dfrac{\Sigma_a SL^2 N\gamma}{4\pi D2(L^2-\Gamma)} \int_o^R \dfrac{e^{-r/L}\, e^{-r/\sqrt{\Gamma}}}{r} 4\pi r^2 dr}{\int_o^R 4\pi r^2 dr}$$

$$\overline{S}_{v_1} = \frac{3\Sigma_a SL^2}{D_2(L^2-\Gamma)4R^3}\left(-LRe^{-R/L}-L^2e^{-R/L}-L^2\right)-\left(\sqrt{\Gamma}Re^{-R/\sqrt{\Gamma}}-\Gamma e^{-R/\sqrt{\Gamma}}-\Gamma\right) \tag{6.29}$$

If the same procedure is applied for thermal flux obtained from removal diffusion theory, the average volumetric gamma source strength will be[xx]

$$\overline{S}_{v_2} = \frac{\Sigma_a N \int_{r_1=o.2}^{R} \left[\dfrac{\sinh Kr}{r} - \dfrac{\Sigma_r S}{8\pi DK} e^{Kr}\left(E_1((\Sigma_r-K)r)-p_1\right)-e^{-Kr}\left(p_1-E_1((\Sigma_r-K)r\right)\right] 4\pi r^2 dr}{\int_{r_1=o.2}^{R} 4\pi r^2 dr} \tag{6.30}$$

$$\overline{SV}_2 = \frac{3N\,\Sigma c}{R^3-r_1^3}\left\{\frac{B}{2}\left[\frac{R}{K}e^{KR}-\frac{1}{K^2}e^{KR}-\frac{r_1}{K}e^{Kr_1}+\frac{1}{K^2}e^{Kr_1}-\frac{R}{K}e^{-KR}-\frac{1}{K^2}e^{-KR}+\frac{r_1}{K}e^{-Kr_1}+\frac{1}{K^2}e^{-Kr_1}\right]\right.$$

$$+\frac{\Sigma_r S}{8\pi DK}\left\{\left(R\frac{e^{KR}}{K}-\frac{e^{KR}}{K^2}\right)E_1((\Sigma r+K)R)-\left(r_1\frac{e^{Kr_1}}{K}-\frac{e^{Kr_1}}{K^2}\right)E_1((\Sigma_r-K)r)-\frac{1}{\Sigma rK}e^{-\Sigma_r R}+\frac{e^{-\Sigma r r_1}}{\Sigma rK}\right.$$

$$\left.-\frac{1}{K^2}E_1(\Sigma_r r_1)+\frac{1}{K^2}E_1(\Sigma_r R)-\left(R\frac{e^{KR}}{K}-\frac{e^{KR}}{K}-\frac{r_1}{K}e^{Kr_1}+\frac{e^{Kr_1}}{K^2}\right)+\left(-R\frac{e^{-KR}}{K}-\frac{e^{-KR}}{K^2}+r_1\frac{e^{-Kr_1}}{K}\right.\right.$$

---

[x] Although the medium is finite, the thermal flux was obtained for an infinite medium, therefore the average volumetric gamma source strength will be somewhat greater than the actual case

[xx] The value of r_1 was chosee so that the thermal flux is finite at that point

$$- \frac{e^{-Kr_1}}{K^2})p_1 - ((- \frac{R}{K} e^{-KR} - \frac{e^{-KR}}{K^2})E_1((\Sigma_r - K)R) - E_1((\Sigma_r - K)r_1)(- \frac{r_1}{K} e^{-Kr_1} - \frac{e^{-Kr}}{K^2}) - \frac{e^{-\Sigma_r R}}{\Sigma_{rK}}$$

$$- \frac{e^{-\Sigma_r r_1}}{\Sigma_{rK}} - \frac{E1(\Sigma_r r)}{K^2} - \frac{E1(\Sigma_r R)}{K^2}\}\} \qquad (6.31)$$

The dose rate from capture gamma at the camera surface is given by

$$D(r) = \frac{\overline{Sv}}{\mu} e^{-\mu_1 d} K \qquad (6.32)$$

where μ is the total linear attenuation coefficient of parafin for gammas of specified energy

μ_1 is total linear attenuation coefficient of stell for gammas of specified enery

K is the dose conversion factor interms of Roentgen

d is steel thickness, 0.5 cm

Dose rates of the camera surface from 2.2 Mev and 4 Mev gamma photons for fixed steel thickness is shown for various camera dimensions Figure 6.10.

The values used in equation 6.32 are given in the appropriate tables.

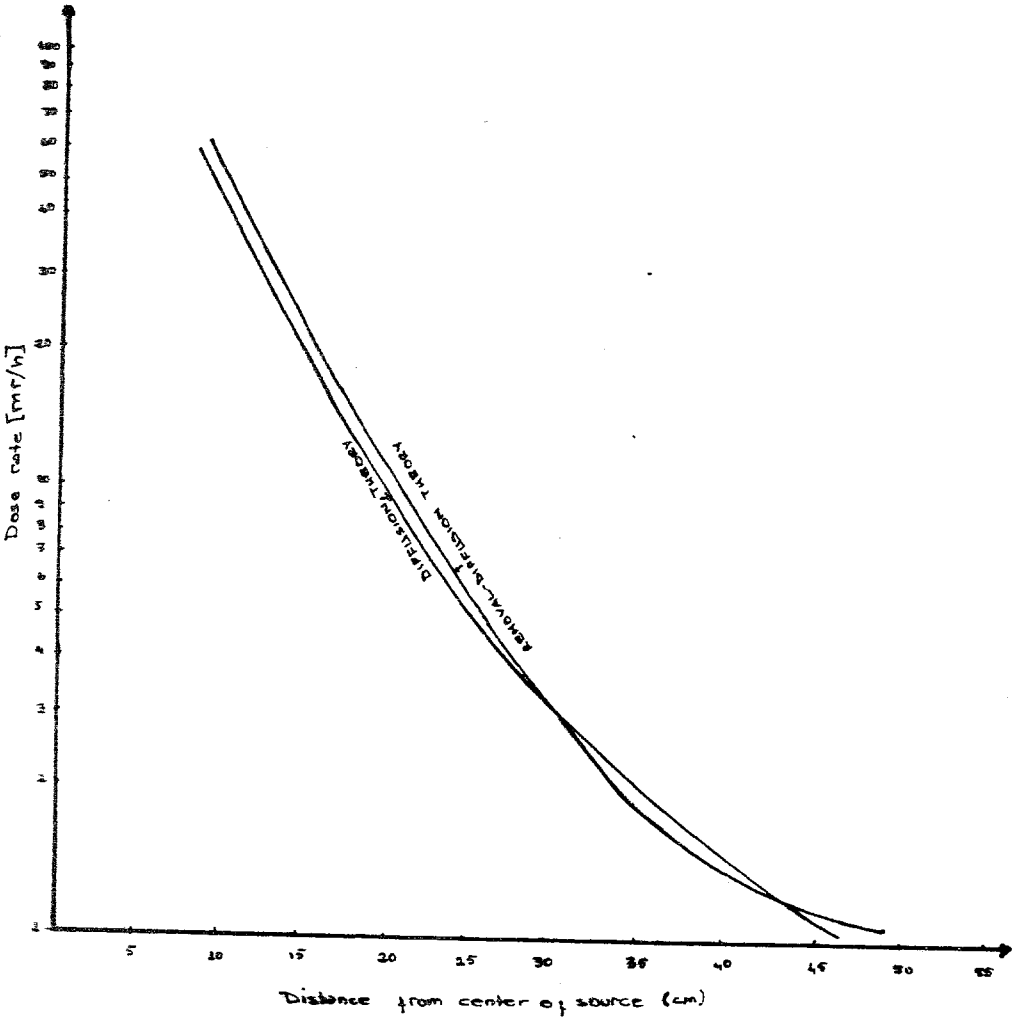

Figure 6.10 The dose rate from capture gammas

Total gamma dose rate at the camera surface is given in Fig. 6.11

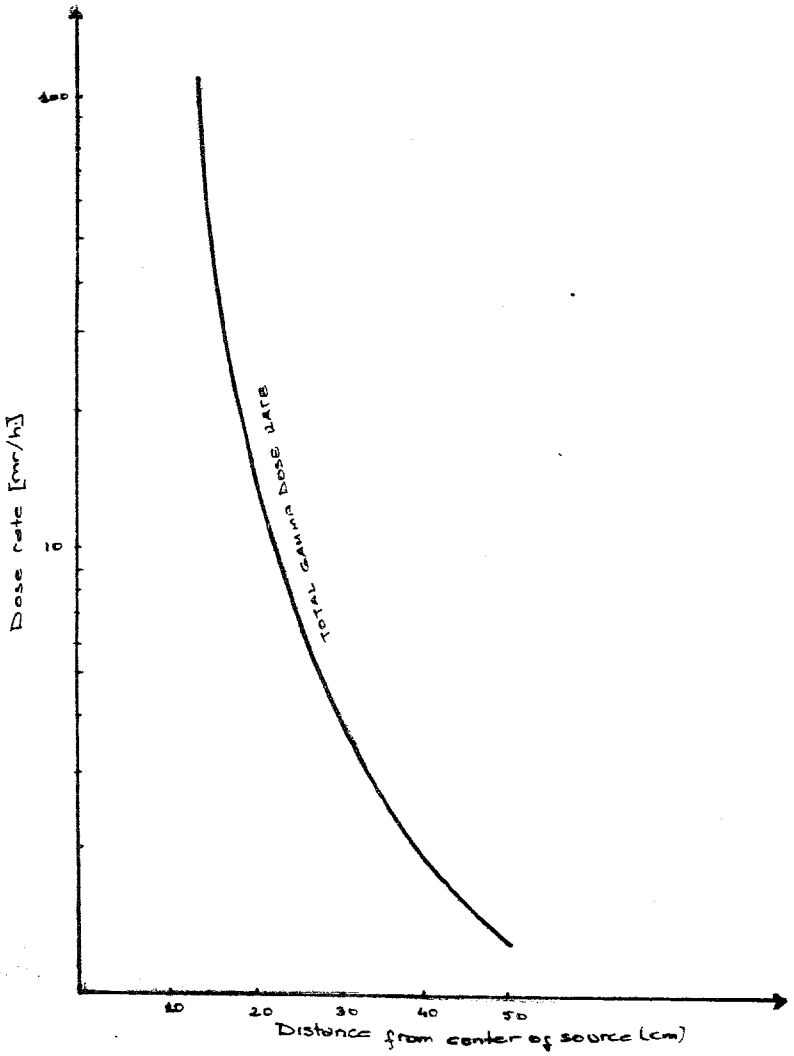

Fig. 6.11 Total gamma dose rate at the camera surface

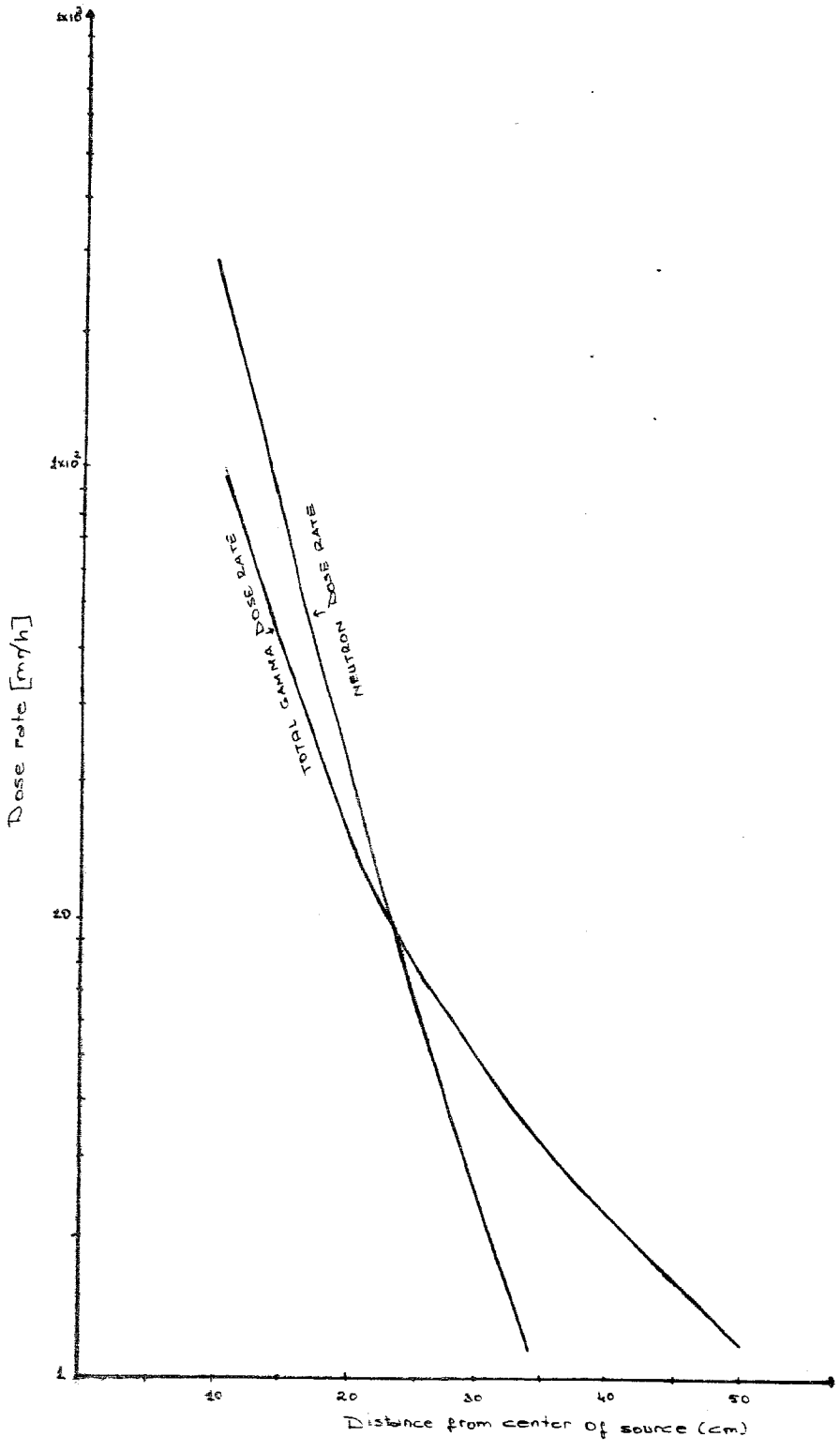

Fig. 6.12 Total gamma and neutron dose rate

CHAPTER VII

DESIGN AND CONSTRUCTION

7.1. Design

Having presented a detailed picture of the principles related to neutron radiography we are now ataposition to design a neutron radiography unit suitable for radiography of a particular range of samples.

Since we have no choice over the type of source and it has a low neutron output we have to use scintillator converter screen, therefore, we can radiography objects for which high resolution is not required.

The moderator dimensions must be such that with source at the center, th addition of extra moderator arround and outside of assembly would'nt be expected to influence the thermal neutron flux at the central region. In other words the moderator assemblies were effectively of infinite radius with respect to central peak thermal flux. This dimension for parafin medium is around 15 cm. However due to shielding considerations, the radius of moderator was chosen as 25 cm to reduce the dose rate as much as possible. To attain a total dose rate of 2.5 mr/hr the radius must be around 35 cm, in which case the camera would be too heavy.

The place of peak thermal neutron flux has been determined and found as 1.5 cm from the source center. To prevent interference of fast neutron and gamma radiation and to increase thermal neutron flux at the image plane, beam extraction position was chosen as tangential rather than radial with a separation of 1.5 cm between the edge of source and the nearest edge of collimator[x].

From the known thermalization factor of around 150[x'] the magnitude of the thermal flux has been determined as 44000 n/cm^{2}sec.

---

[x] The same considerations apply for ^{241}Am-^{242}Cm-Be source experimentally except that a separation between the edge of the source and the nearest edge of collimator of 2 cm out to be the optimum arrangement (27)

[x'] This value of thermalization factor is rounded value.

Two collimators have been made with cadmium, with dimensions of 4 cm diameter x 25 cm lenght and 3 cm diameter x 25 cm length. The thickness of collimator wall has been calculated from

$$C=1-e^{-\Sigma t}$$

where

C = the attenuation factor

Σ = the macroscopic absorbtion cross section of cadmium cm^{-1}

t = the thickness of collimator wall

The calculated thickness is 0.2 mm and is sufficient to make attenuation factor equal to 0.95. The thickness of collimator wall used is about 1 mm.

Air-gap fine turning has been considered and the unlined lenght of collimator was taken as five cm

The expected thermal neutron flux at the image plane in case of two collimators has been calculated as 98 n/cm^2 for 4 cm diameter and 55 n/cm^2 for 3 cm diameter.

7.2. Construction

Although thermal neutron flux distribution and dose rates have been calculated for spherical geometry, difficulty of constraction of a spheric has led to a preferance of cylindirical shape for the camera. The spheric with the radius of 25 cm is the largest sphere that fits into the cylindir.

The cylindir has been made from St 37 steel. The central source port has been made from a P.V.C. pipe of 4 cm india. Parafin was then melted and poured in to the cylinder. Collimator have been made in trancated conical shape from cadmium. The camera has been painted to protect it from currision. For case of transportation three wheels has been incorporated to the camera.

The total weight of camera is about 121 kg.

To handle sample and film casete an image handle have been made The detail drawing of camera is given in Figure 7.1 and a photograph of system is given by in Figure 7.2

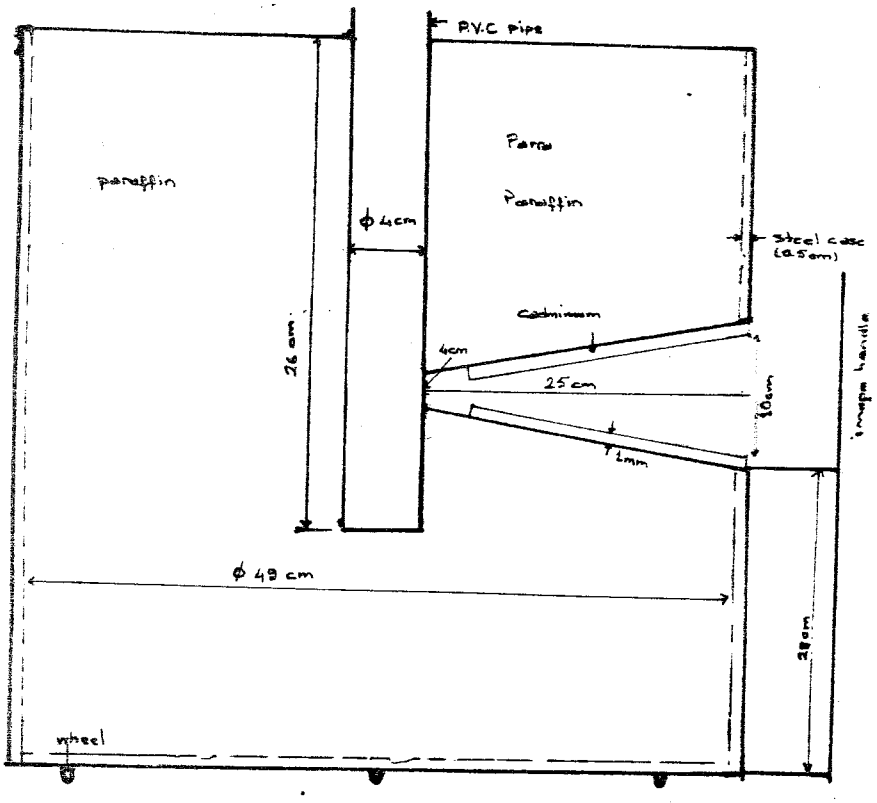

Fig. 7.1. Detailed drowing of camera

7.3. Application

A radiography of a cadmium resolution indicator, a rubber o-ring wrapped in alaminium tape, and a piece of printed circuit was taken using direct technique with a gadolinium back screen.

Figure 7.4 is a positive of the neutron radiography of these objects. Type 0.7 film was used with an exposure time of 28 hours at a thermal beam flux of 45 $n/cm^2 sec$. The film density produced by the unattenuated thermal neutron beam was measured as 1.5.

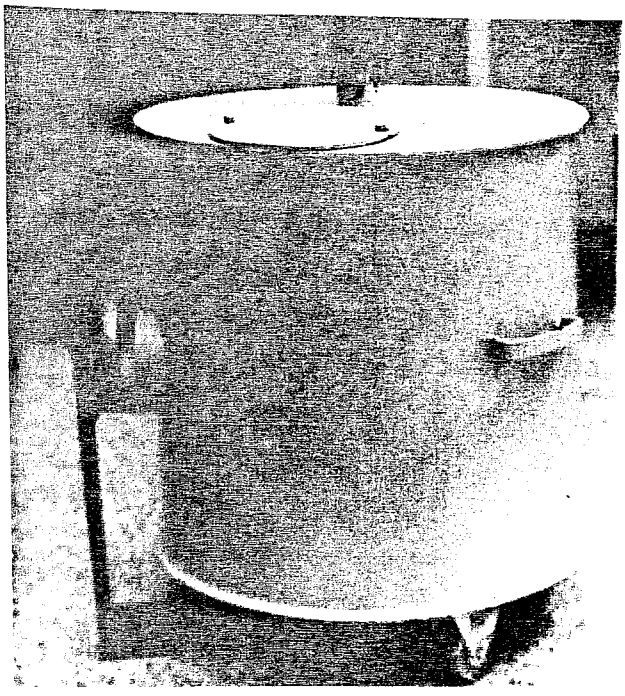

Fig. 7.2. Neutron radiography facility

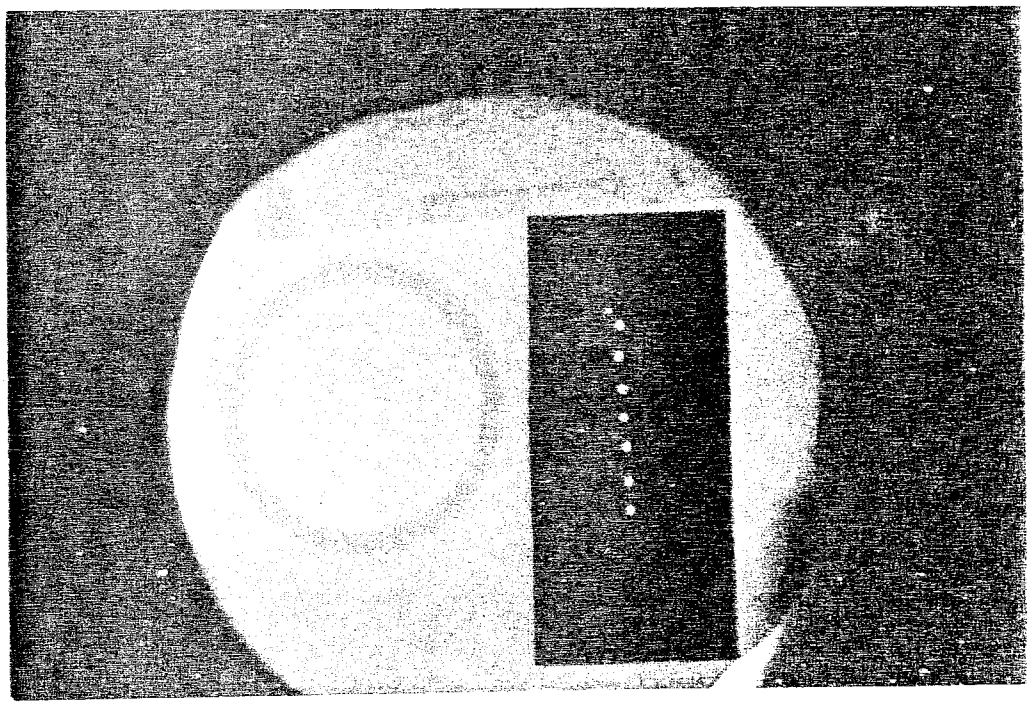

Fig. 7.3. Neutron radiograph using Gadolinium converter screen with Type D7 film. The specimens are a cadmium resolution indicator a rubber o-ring wrapped in alaminium tape, and a piece of printed circuit.

CHAPTER VIII

DISCUSSION AND CONCLUSIONS

Big investment requirements for precurement of a nuclear reactor for neutron radiographic applications led to a preference of neutron radiography facilities that uses radicactive and accelerator neutron sources. These facilities are useful especially for applications that require mobility, modest resolution, and long exposure times.

A starting point for the development of such facility a neutron radiographic camera containing, 3 curi ^{241}Am-Be neutron source, available in laboratory for research purposes, has been designed and constructed.

Since the output of ^{241}Am-Be source is low, efforts have been concentrated on designing a camera which produces as high a thermal flux at the image plane as possible. Mean while shielding requirements and weight of the camera have been also considered.

To calculate the thermalization factor, the position of peak thermal flux and the dimension of moderator which acts effectively as an infinite medium a theoretical analysis has been made in three different ways.

It will be seen from Table 6.3 that the thermalization factors obtained are lower than the values experimentally determined, which is arround 200 for water moderator. The factors leading to such a low values are the assumption of a point source and thermalization of all the removed neutrons. It can be seen from Table 6.3 that the thermalization factor obtained with removal age theory, in which case source is not considered as a point source and allowance are made for tehrmalization of neutrons through age theory, is greater than the values obtained with the other two methods.

Through the use of removal-diffusion theory it has been determined that for thicknes greater than 110 cm the parafin acts as infinite medium for the central peak of thermal neutron flux.

The calculated dose rate acoording to the methods indicated in chapter six fits closely the measured values and indicates that aradius of 35 cm is necessary to decrease the dose rate to 2.5 mr/hr.

The weight of camera with this radius would be 332 kg which is high for a mobile unit. Therefore a compromise has been made between the dose rate and the weight so as to choose a radius of 25 cm. The dose rate at the surface of the camera with this radius is arround 15 mr/hr. This value of the dose rate is within in the shipment limits. For mobility, and as a precaution during operation a prohibitive line is to be placed arround the camera in which case the dose rate will be reduced to 2.5 mr/hr.

Calculated thermal flux at the collimator exit with a thermalization factor of 108 in the case of 4x28, and 3x25 cm collimators are 109 and 77 n/cm^2sec respectively.

However the measured value of thermal neutron fluxes at the collimator exit are the same and equals to 45 n/cm^2sec. This value of thermal flux fits the value obtained when thermalization factor is taken as 200. In this case the thermal flux at the exit of collimator will be 58 n/cm^2-sec and 42 n/cm^2-sec respectively.

Since the value of thermal flux at the image plane is too low NE 421 scintillator converter will be used as converter screen and because of low collimator ratio of radiographic unit, thin objcets will be radiographed.

REFERENCES

1. Garrett,D.A.,Berger,H.,"The Technological Development of Neutron Radiography,"Atomic Energy Review,Vol.15,pp.125-129,1977.
2. Barton,J.P.,"Neutron Radiography An Owerview,"Neutron Radiography and Gaging,"ASTM Publications,1975.
3. Hawkeswort,M.R.,"NeutronRadiography Equipment and Methods,"Atomic Energy ReviewVol.15,No.2,pp.169-216,1977
4. Barton,J.P.,"Neutron Sources for Neutron Radiography,"Radiography with Neutrons,Proceedings of aconference held 10-11,September1973 London pp.7-13 Brt.Nuc.En.Soc.1975.
5. Berger,H., Neutron Radiography, Elsevier Publishing Comp.,New York 1965.
6. Vasilik,D.G.,"Thermal Neutron Radiography with Sealed Tube Neutron Generator and Water Moderator,"Nuclear Technology,Vol.14,No.3,pp.279-283,January 1972.
7. Numec, Pulutonium Beryllium Neutron Source,Apollo Pensilvania.
8. Engineering Compendium on Radiation Shielding,Shielding Fundemantals and Methods, New York,1976.
9. Profio,A.E.,Experimantal Reactor Phsics,Wiley Interscience Publication, New York,1976.
10. Vonderhardt,P.and Rotter,H.,Neutron Radiography Hand Book,D.Reidel Publishing Company,London,1981.
11. Barton,J.P.,"Divergent Beam Collimator for Neutron Radiography," Materials Evaluation,Vol.15,No.9,pp.45A-46A,September 1967.
12. Barton,J.P.,"Developments in Use of Californium-252 for Neutron Radiography,"Nuclear Technology,Vol.15,No.1,pp.56-67,july 1972.
13. Barton,j.P.,"^{244} Cm and ^{252} Cf for Neutron Radiography,"Tran.Am.Nuc. Soc.,Vol.14,No.2,pp.516-517,1971.
14. Berger,H.,"Comparison of Several Methods for the Fotographic Detection of Thermal Neutron Images,"Journel of Applied Physics,Vol.33,No.1,pp.48-56,January 1972.
15. Kelly,D.,Nicoll,D.,"Scintillator Screens for Neutron Radiography," Radiography with Neutrons,Proceedings of a conference held 10-11 september 1973,Brt.Nuc.En.Soc.,1975.
16. Berger,H.,"Detection Systems for Neutron Radiography,"Neutron Radiography and Gaging,ASTM,Publications 1975

17. Berger,H.,"Resolution Study of Photographic Thermal Neutron Image Detectors,"Journal of Applied Physics,Vol.34,No.4,pp.914-918,April 1963.

18. Hendry,I.C.,"A Neutron Radiography Unit Based on (D,T) Neutron Generator,"The Int.Jor.of Appl.Rad and Iso.,Vol.20,No.6,Jun 1963-

19. Berger,H.,"Improved Sensitivity and Contrast for Trac Etch Thermal Neutron Radiography,"Trans.Am.Nuc.Soc.,Vol.15,No.1,pp.123,June 1972.

20. Durrani,S.A.and Khan,H.A.,"Solid State Track Detectors for Neutron Image Recording,"Proceedings of a conference held 10-11,September 1973,London,pp.71-77,Brt.Nuc.En.Soc.1975.

21. Berger,H.,"Charecteristics of a Thermal Neutron Television Imaging System,"Materials Evaluation,September 1966.

22. Spowrt,A.P.,"Mobile Unit for Neutron Radiography,"Nuclear Engineering, pp.429-431,May 1968.

23 Hawkeswort,M.R.,"Radiography with Neutrons,"Journal of Materials Science Vol.4,pp.817-835,May 1969

24. Hawkesworth,M.R.,"Neutron Image Recorders,"Radiography with Neutrons Proceedings of a conference held 10-11 September 1973,London Brt.Nuc.En.Soc.,L975.

25. Barton,J.P.,"Devolepment of Neutron Radiography Applications in the U.S.A,"Radiography with Neutrons,Proceedings of a conference held 10-11 September 1973,London,pp.157-163,Brt.Nuc.En.Soc.,1975.

26. Radioactive Product,The Radiochemical Center,Amersham,1970

27. Barton,J.P.,"Experiments with ^{241}Am-^{242}Cm-Be for Neutron Neutron Radiography,"Materials Evaluation,Vol.30,No.11,November 1972.

28. ANL-5800.,Reactor Physics Constants.

29. Glasstone,S.,Sesonske,A.,Nuclear Reactor Engiinering,D.Van Nostrand Company.,1963.

30. Lamarsh,J.R.,Introduction to Nuclear Reactor Theory,Addision -Wesly Publishing Company,1972.

31. Bennet,I.G.I.,"^{252}Cf Neutron Radiographic Camera,"Radiography with Neutrons,Proceedings of aconference held10-11 September 1973,London, Brt.Nuc.En.Soc.,1975,pp.45-47.

32. Goldstein,Fundemantal Aspects of Reactor Shielding,Addision Wesley Publishing Company,1959,New York

33. Engineering Compendium on Radiation Shielding,Shielding Fundemantals and MethodsII,New York,1968.

34. Price,B.T,,Sanny,K.T.,Radiation Shielding,Pergoman Press,1957.

35. Valenta, F.A.,A manual of Experiments in Reactor Phsics,The Macmillian Company,New York,1963.

36. Etherington,H.,Nuclear Engiinering Handbook,Mc Graw Hill Company,1958.